A Multi-wavelength View of Galaxy Cluster Scaling Relations

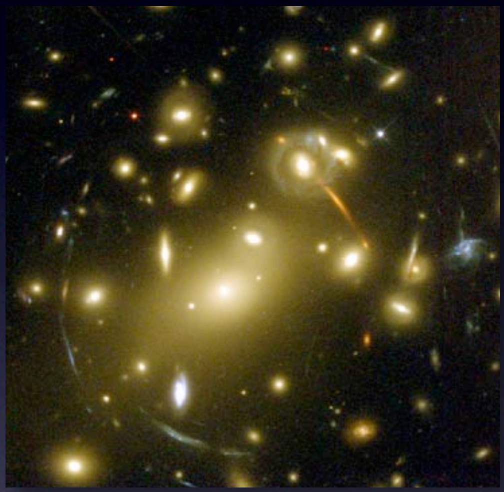

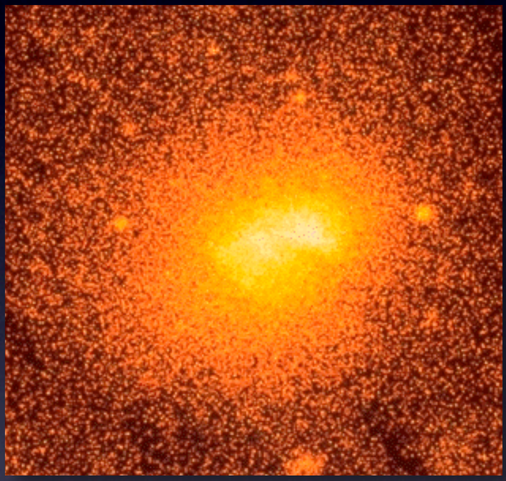

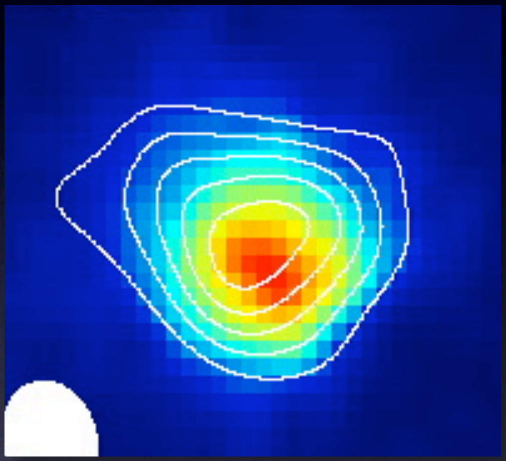

August (Gus) Evrard
Arthur F. Thurnau Professor
Departments of Physics and Astronomy
Michigan Center for Theoretical Physics
University of Michigan


Collaborators:
Eduardo Rozo
Eli Rykoff
Jim Bartlett
(+ 3 X-ray groups)
KITP Workshop
Galaxy Clusters: The Crossroads
of Astrophysics and Cosmology
January 31 – April 22, 2011

basic ingredients for cluster cosmology from counts + clustering

1. halo space density (aka, *mass function*), $dn(>M, z)/dV$
   - well calibrated (~5% in d*n*) by (dark matter only) simulations

2. two-point spatial clustering of halos (aka, *bias function*), $b(M, z)$
   - similarly well calibrated

3. population model for signal, S, used to identify clusters, $p(S \mid M, z)$
   - power-law with log-normal deviations (typically self-calibrated)
   - projection effects (signal-dependent) $S_{\mathrm{observed}} \neq S_{\mathrm{intrinsic}}$

4. selection model for signal, S
   - completeness (missed clusters)
   - purity (false positives)

observable signal choices for surveys: pros and cons

Signal	Pros	Cons
X-ray	• spatially compact signal (relative to other methods) • hot thermal ICM is unique to clusters • 40+ year science history	• expensive (space-based) • flux confusion from AGN • surface brightness dimming • most sources will have moderate S/N
Optical	• inexpensive (*free* with any galaxy survey!) • old, `red sequence' galaxies reside in massive halos • 80+ year science history	• confusion from line-of-sight projection • moderate S/N (Poisson statistics for $N \geq 10$) • galaxy formation!
Sunyaev-Zel'dovich	• inexpensive (*free* w/ resolved, multi-band CMB survey) • nearly redshift-independent signal	• point source confusion • l-o-s projected confusion with low angular resolution • moderate S/N for most

cluster samples today are sparse relative to massive halos on the sky

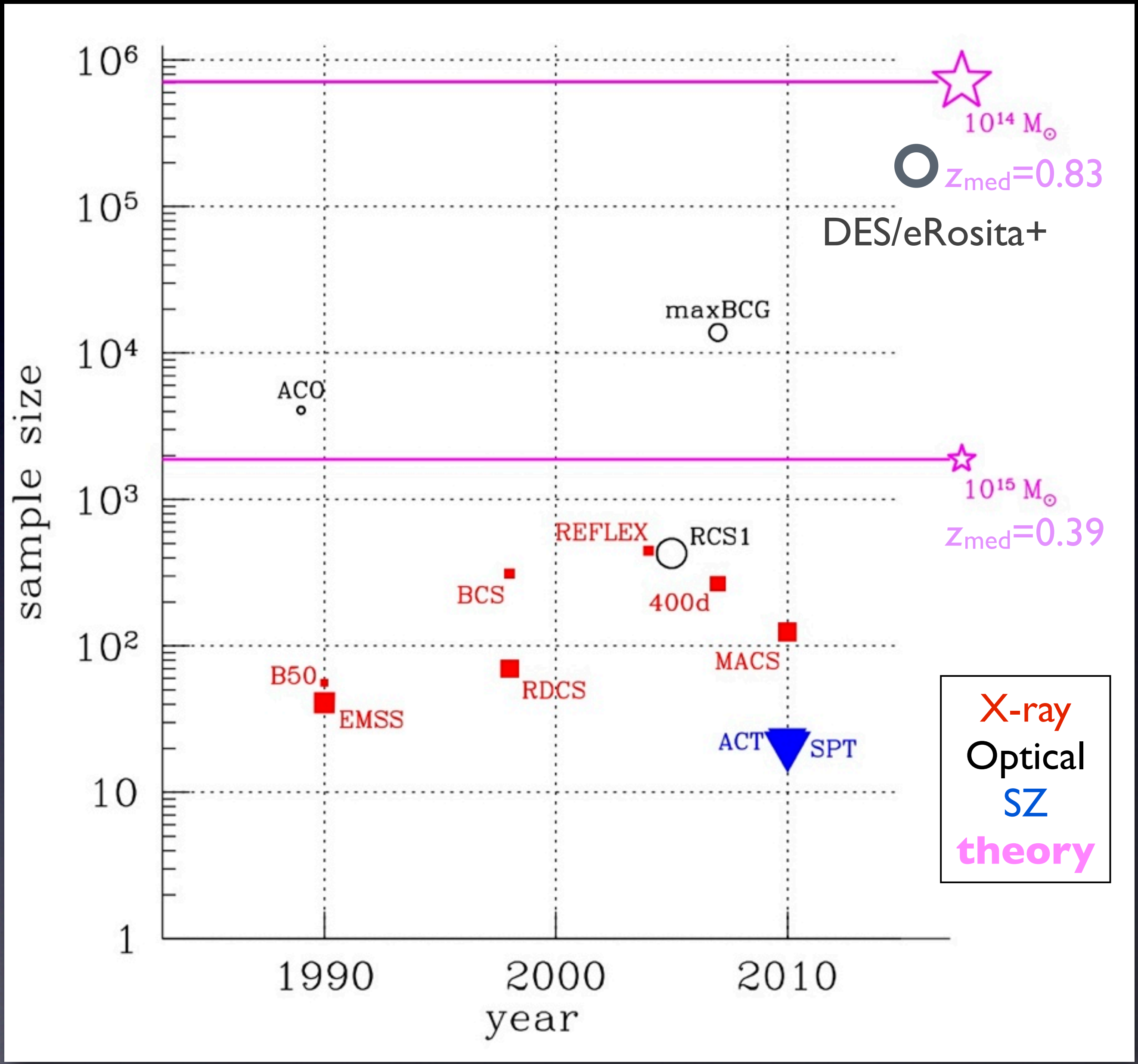

Allen, Evrard & Mantz 2011

symbol size scales with median redshift

Halo mass scale is M_{200m} (h = 0.7)

a prototypical `relaxed' cluster

Allen, Evrard & Mantz 2011

Abell 1835 (z=0.25) seen in X-ray, optical and mm bands

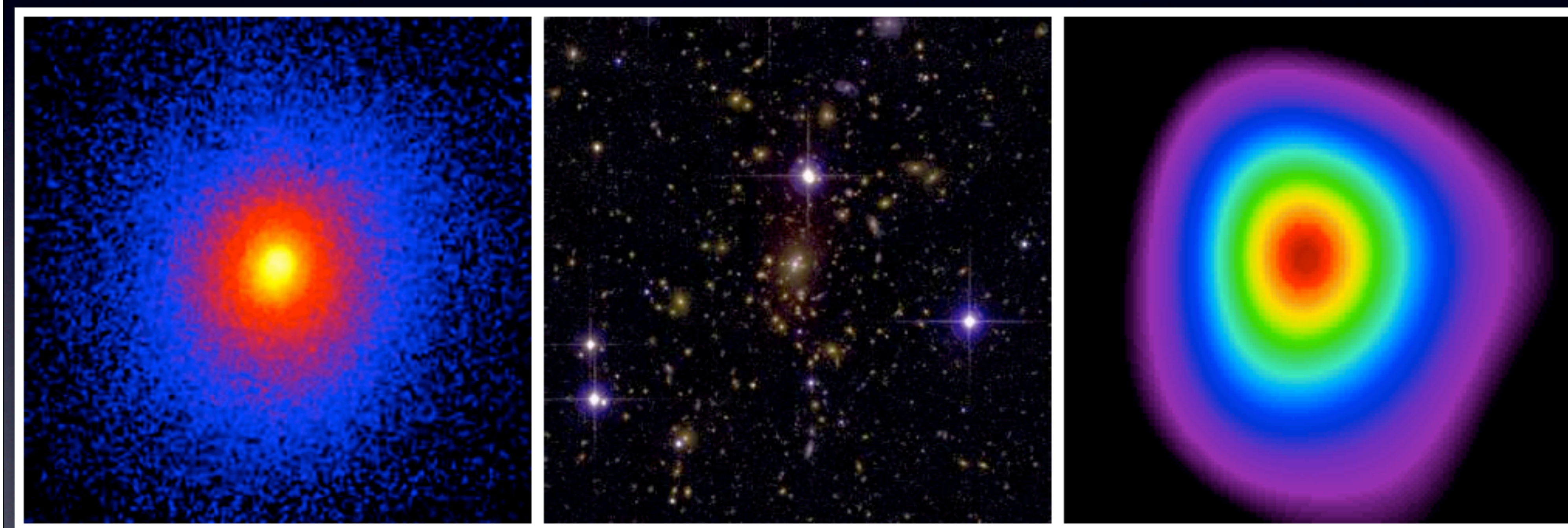

1.2 Mpc

an extreme `train wreck'

Jee et al 2012

Abell 520 (z=0.20) seen in X-ray, optical w/ lensing mass contours

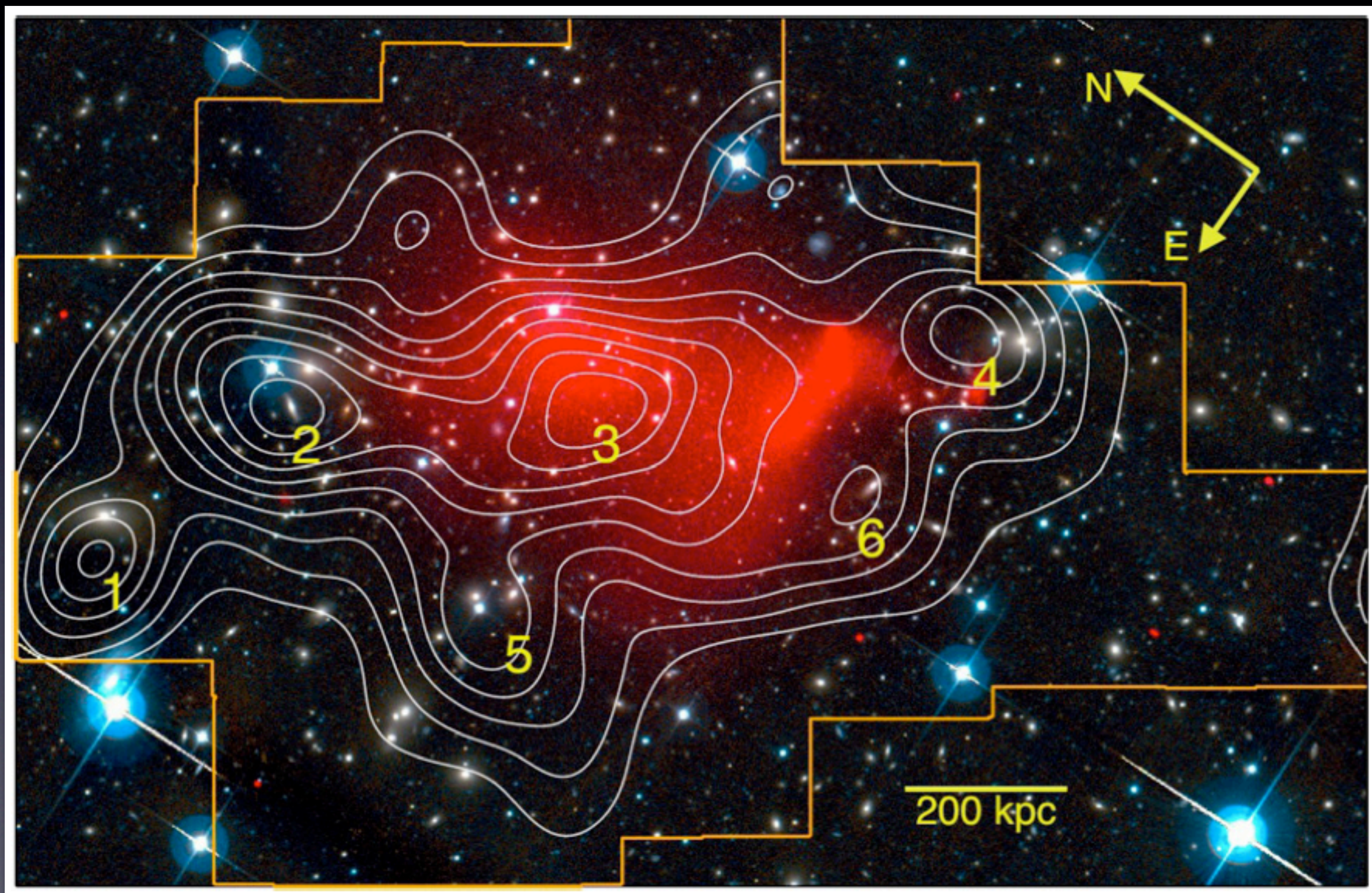

consistent cosmology from existing optical and X-ray samples

Rozo et al 2010

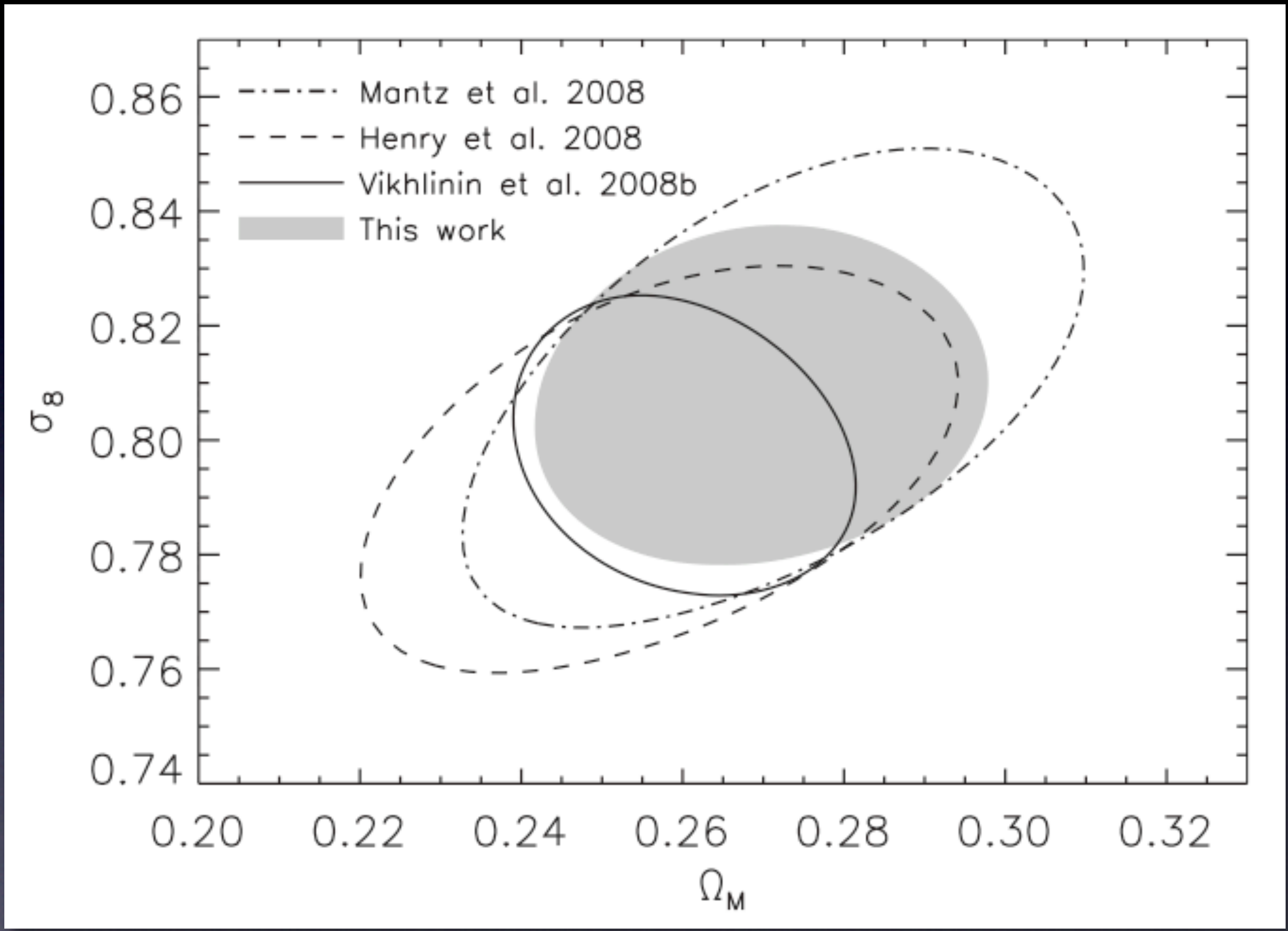

optical: maxBCG
(shaded)
~14,000 clusters

X-ray: 400d, BCS
(lines)
~100 clusters

systematics limited !

how hard is counting? Major systematic error sources for cluster cosmology

1. 3D halo mass is not directly observable
   – what is the form of the intrinsic signal likelihood, $p(\boldsymbol{S}_{\rm int} \mid M, z)$?

2. $\boldsymbol{S}_{\rm int}$ is also not directly observable (the universe is a big place!)
   – how does ~Gpc sight-line projection distort $\boldsymbol{S}$?
   – what is the impact on survey selection ?

3. Baryons (17% of matter) are dynamically complex on Mpc scales
   – do mergers lead to strong selection biases?
   – does feedback excite decaying modes on quasi-linear scales?

surprise from Planck stacking of optically-selected (maxBCG) clusters

Planck Collaboration arXiv:1101.2027

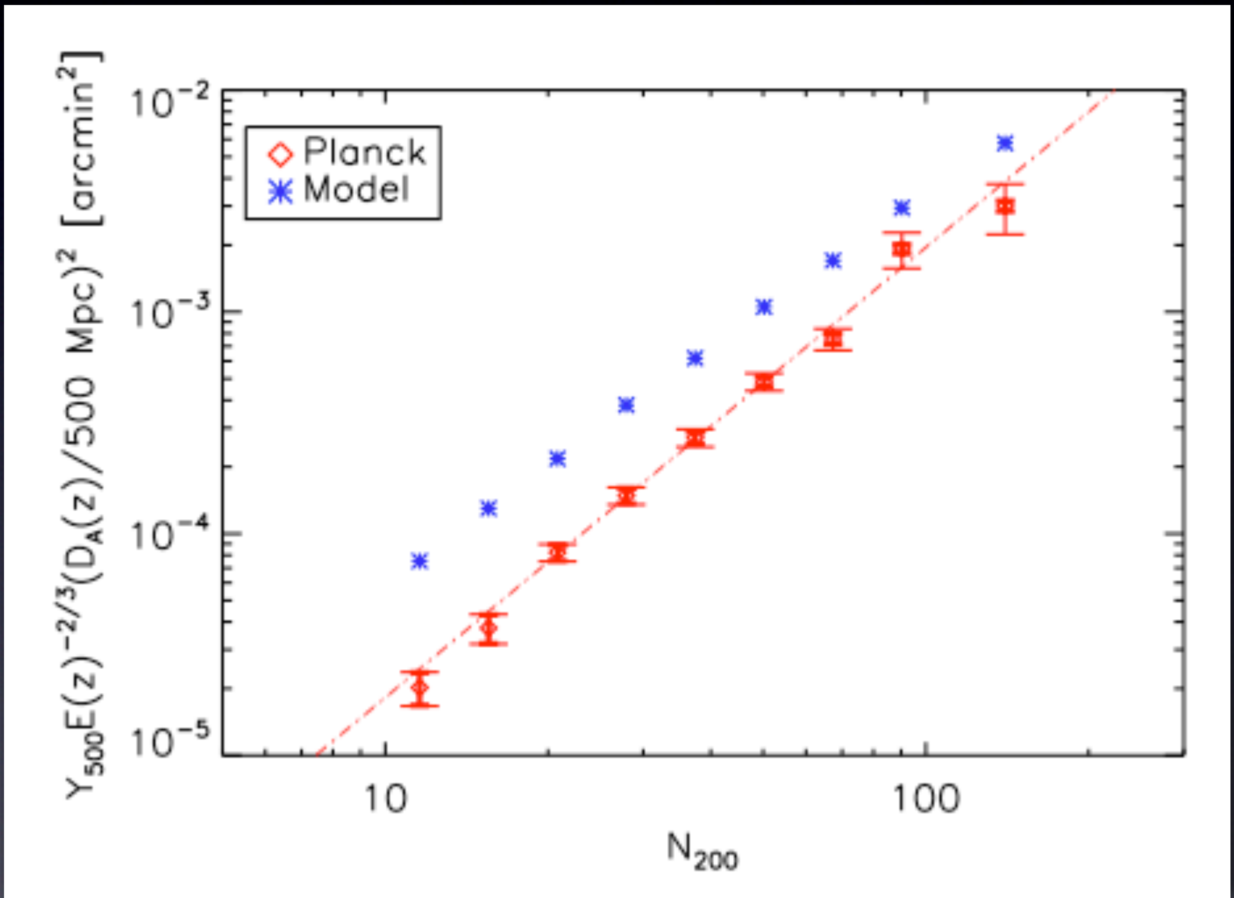

SZ decrement in maxBCG cluster sample is smaller than ***model prediction*** by factor >2

Planck model : steps from Ngal to Ysz

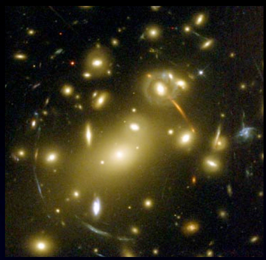

=> M_{lens} ? = $M_{X\text{-ray}}$ =>

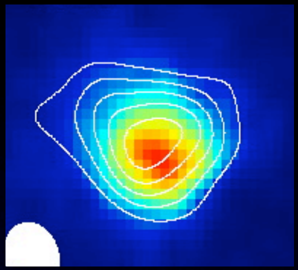

optical Ngal

lensing mass

X-ray hydrostatic mass

thermal SZ amplitude

|| M_{true}?

* masses from stacked weak lensing analysis
* optically-selected sample
* based entirely on SDSS data

* masses assume hydrostatic equil'm of hot gas
* X-ray selected samples
* based mainly on XMM data
* assumes Yx = Ysz (Yx = Mgas * Tx)

paper I:
comparison of published
cluster properties
from X-ray observations

comparison of published **total mass** (M_{500c}) estimates for local galaxy clusters

Rozo et al (2012) arXiv:1204.6301

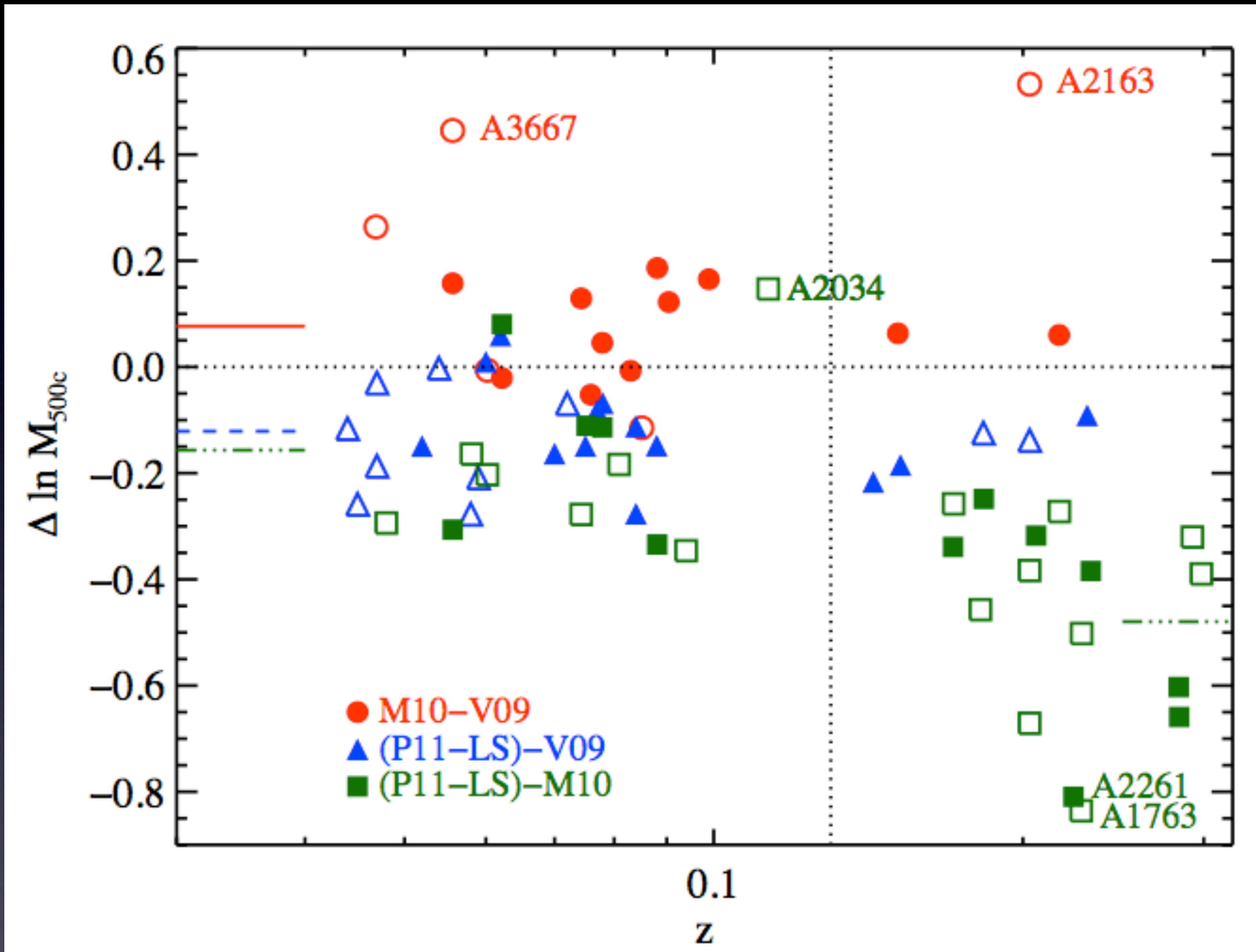

y-axis shows

$\ln(M_A / M_B)$

for samples A–B listed in legend

M10: Mantz et al (2010)
V09: Vihklinin et al (2009)
P11-LS: Planck Coll. (2011)

median published statistical error ~5%

filled: cool core/relaxed
open: non-cool core/unrelaxed

comparison of published **gas mass** estimates for local galaxy clusters

Rozo et al (2012) arXiv:1204.6301

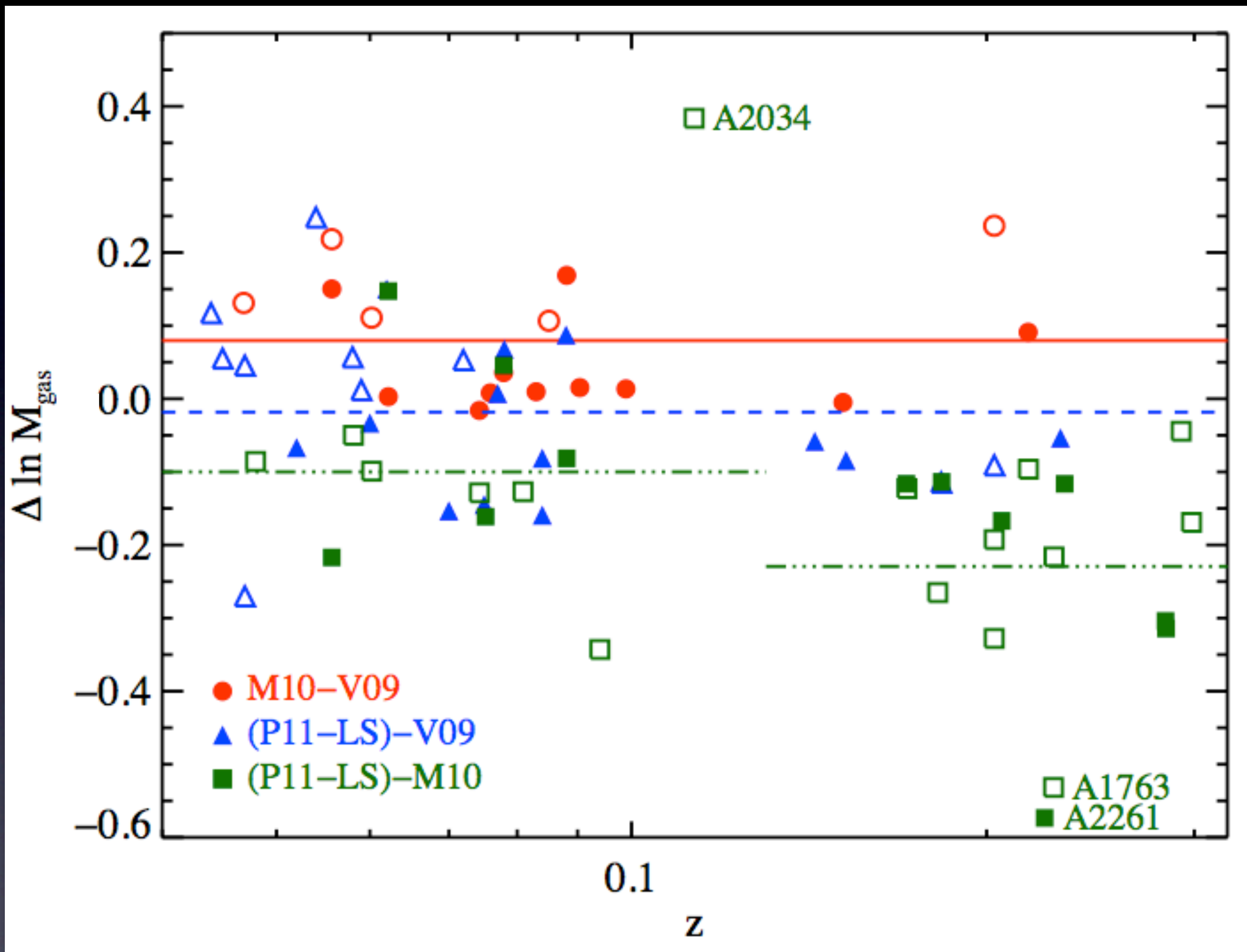

similar pattern to total mass estimates reflects *aperture-induced bias*

M10: Mantz et al (2010)
V09: Vihklinin et al (2009)
P11-LS: Planck Coll. (2011)

filled: cool core/relaxed
open: non-cool core/unrelaxed

comparison of published **gas mass** estimates for local galaxy clusters

Rozo et al (2012) arXiv:1204.6301

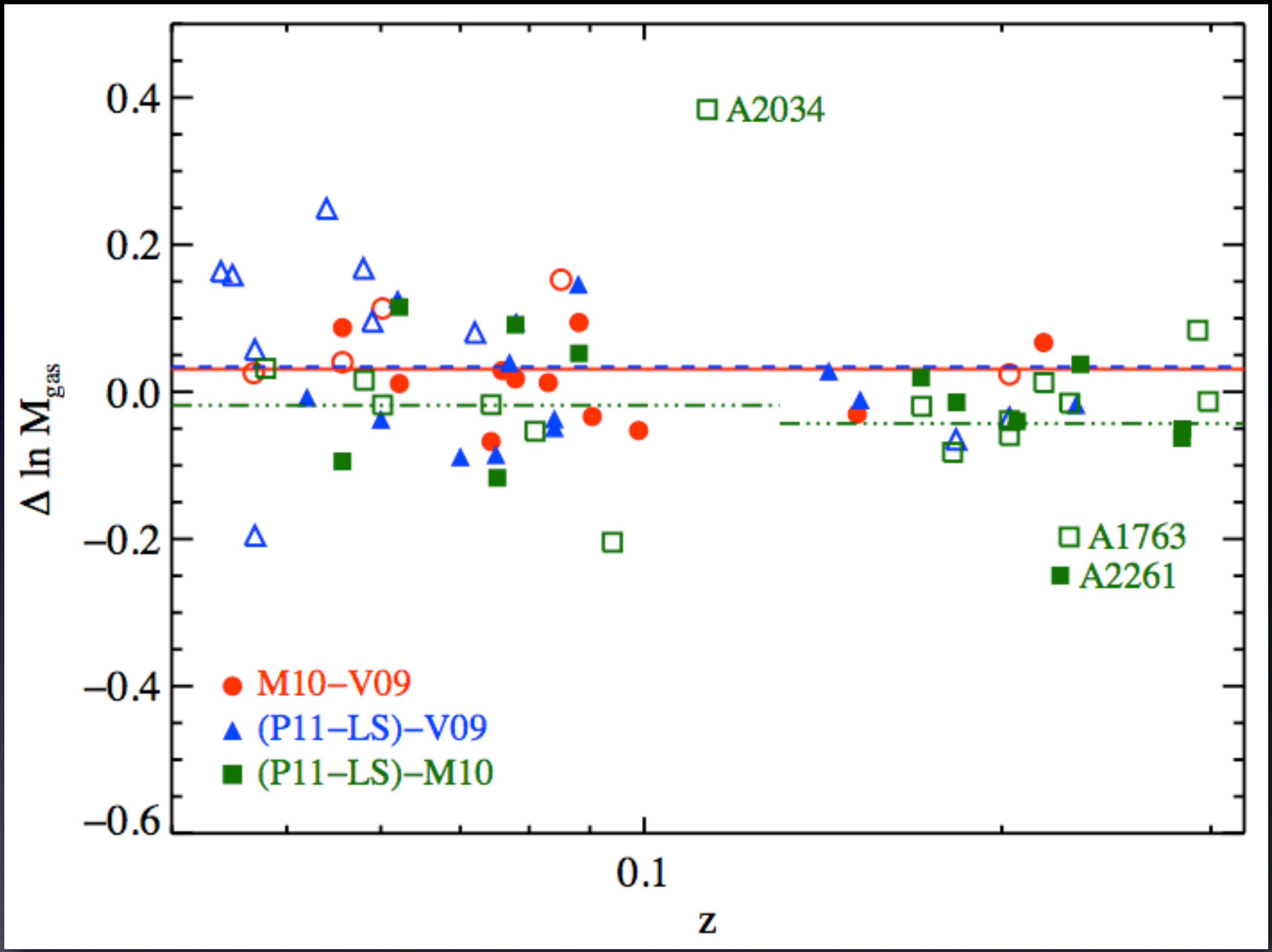

good agreement after correcting to common radial aperture

M10: Mantz et al (2010)
V09: Vihklinin et al (2009)
P11-LS: Planck Coll. (2011)

filled: cool core/relaxed
open: non-cool core/unrelaxed

comparison of published **gas temperature** estimates for local galaxy clusters

Rozo et al (2012) arXiv:1204.6301

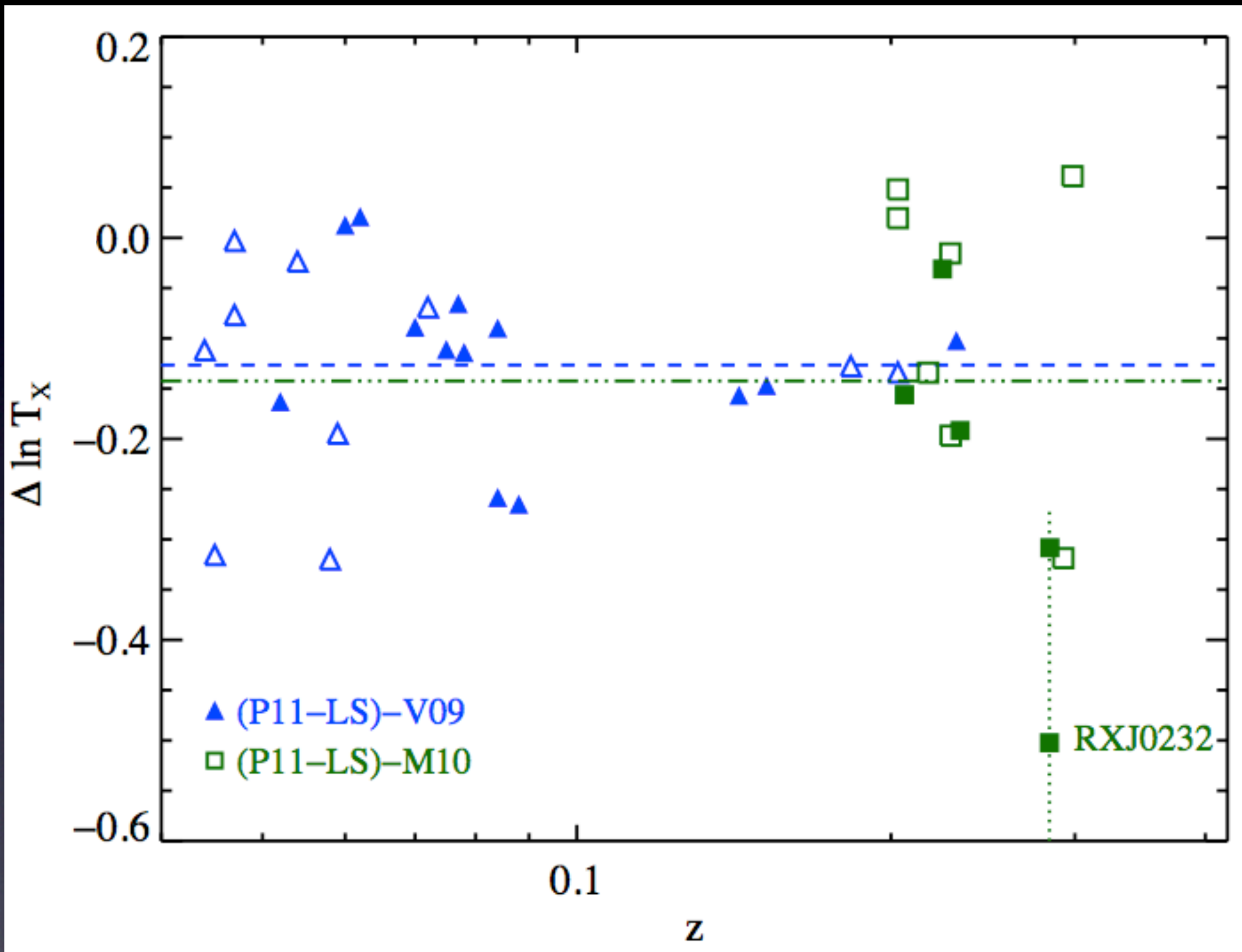

fewer **independent** estimates of Tx (need long exposures) => no M10-V09 comparison

M10: Mantz et al (2010)
V09: Vihklinin et al (2009)
P11-LS: Planck Coll. (2011)

filled: cool core/relaxed
open: non-cool core/unrelaxed

comparison of published **gas thermal energy** estimates (Yx = Mgas * Tx)

Rozo et al (2012) arXiv:1204.6301

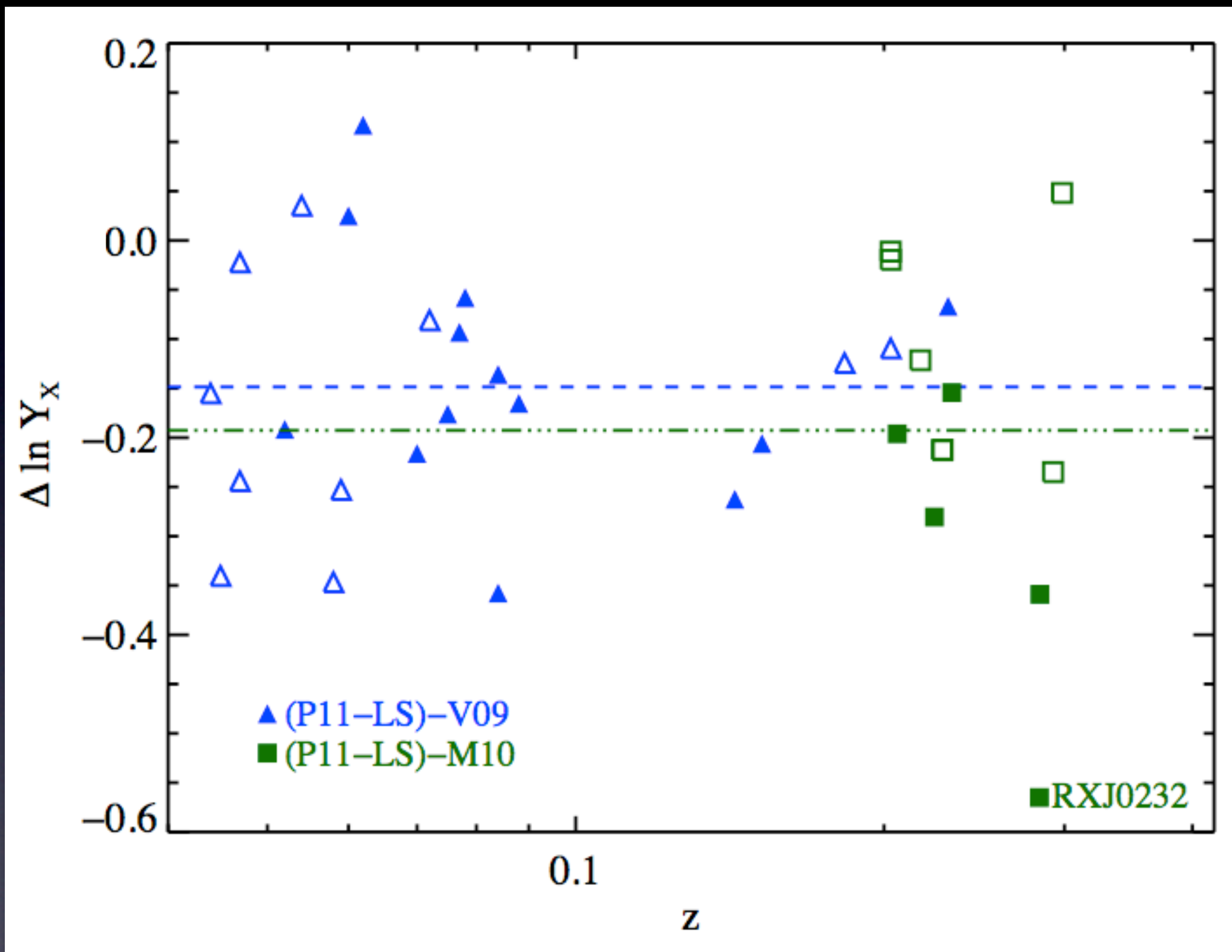

comparison is shown **after** correcting Mgas to common aperture

M10: Mantz et al (2010)
V09: Vihklinin et al (2009)
P11-LS: Planck Coll. (2011)

filled: cool core/relaxed
open: non-cool core/unrelaxed

comparison of published properties for local galaxy clusters : summary table

Rozo et al (2012) arXiv:1204.6301

Mean Log Differences in X-ray Properties for Sample Pairs

Property	M10 – V09	P11-LS – V09	P11-LS – M10 Low z ($z \leq 0.13$)	P11-LS – M10 High z ($z > 0.13$)
L_X [a]	0.12 ± 0.02	-0.01 ± 0.02	-0.12 ± 0.02	-0.10 ± 0.03
M_{gas} [a b]	0.03 ± 0.02	0.03 ± 0.02	-0.02 ± 0.03	-0.04 ± 0.02
T_X	—	-0.13 ± 0.02	—	-0.14 ± 0.05
Y_X [a b]	—	-0.15 ± 0.03	—	-0.19 ± 0.05
M_{500} [c]	0.08 ± 0.02	-0.12 ± 0.02	-0.16 ± 0.07	-0.48 ± 0.07
M_{500} [d]	0.22 ± 0.11	-0.14 ± 0.03	-0.25 ± 0.03	-0.45 ± 0.06

[a] Offset computed after outlier removal.
[b] Offset computed after correction to a common aperture.
[c] Relaxed/cool core only.
[d] Non-relaxed/no cool core only.

Note: post-publication, M10 masses were subsequently adjusted downward by 11% due to Chandra recalibration

M10: Mantz et al (2010)
V09: Vihklinin et al (2009)
P11-LS: Planck Coll. (2011)

comparison of published **gas thermal energy** estimates (Yx = Mgas * Tx)

Rozo et al (2012) arXiv:1204.6301

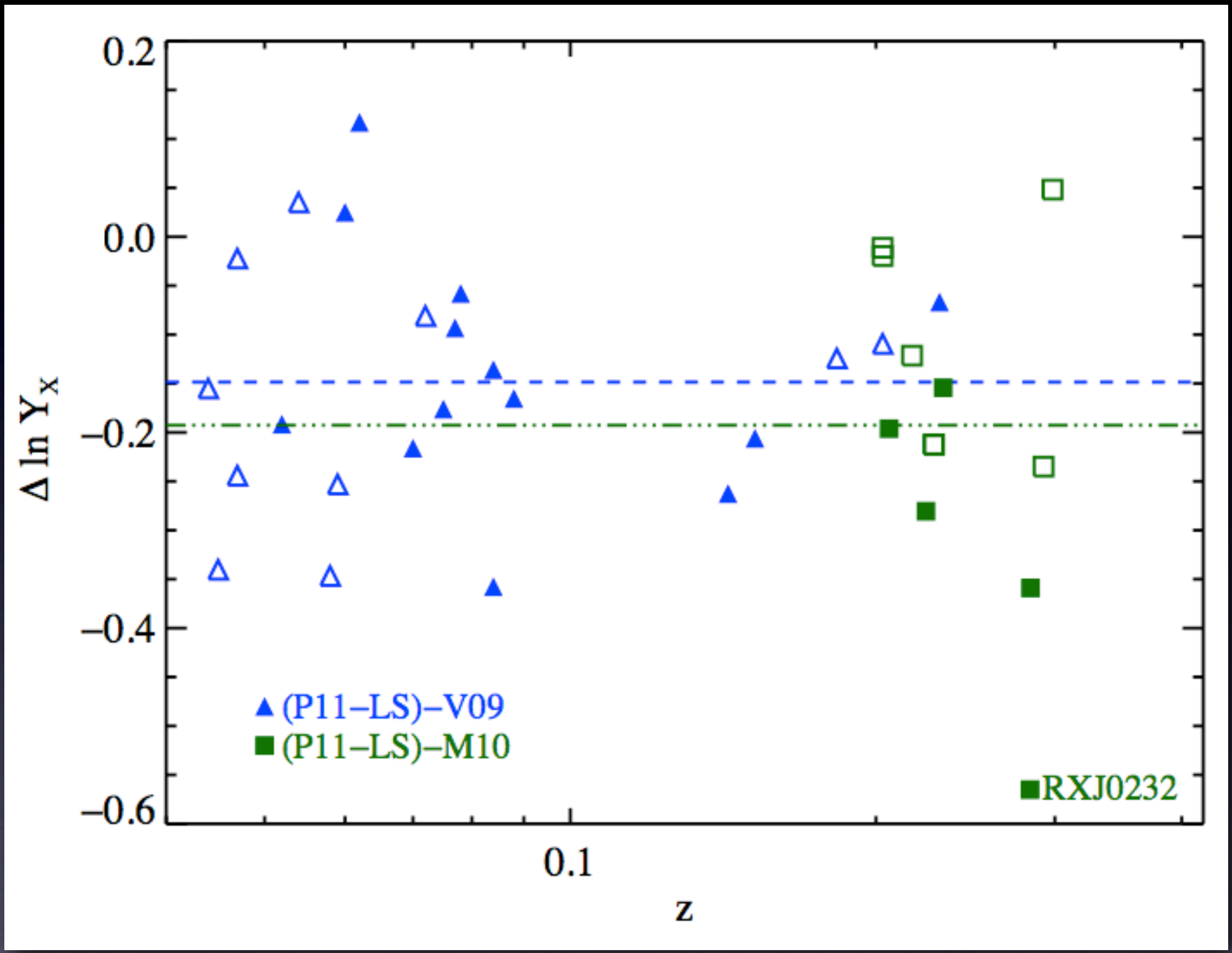

comparison is shown **after** correcting Mgas to common aperture

M10: Mantz et al (2010)
V09: Vihklinin et al (2009)
P11-LS: Planck Coll. (2011)

filled: cool core/relaxed
open: non-cool core/unrelaxed

paper I summary

- X-ray projects derived 3D halo mass implicitly from scaling relations

  M_{gas}-M_{tot} (M10) ; Y_X-M_{tot} (V09) ; Y_X-M_{tot} (P11)

  - calibrated by $M_{hydrostatic}$ small number (~10's) of relaxed clusters with assumption $M_{hydrostatic} = M_{tot}$
  - systematic variations ~few 10's of percent exist in M_{tot} estimates

- observed cluster properties ($<R_{500}$) from 3 groups vary
  - mainly due to aperture bias (different R_{500} estimates)
  - M_{gas} shows best agreement after aperture correction
  - Y_X is worst (T_X estimates vary in mean)
  - largest tensions between P11-LS and M10 at z>0.13

paper II:
comparison of published
X-ray scaling relations
+
a log-normal
multivariate model
for consistency checks

published relations of Lx-M, Yx-M and Ysz-Yx

TABLE 1
INPUT CLUSTER SCALING RELATIONS AT $z = 0.23$

Relation	χ_0	a	α	$\sigma_{\ln\psi\vert\chi}$	Citation	Data Set
L_X–M_{500}	4.8	1.16 ± 0.09	1.61 ± 0.14	0.396 ± 0.039	Vikhlinin et al. (2009)	V09
L_X–M_{500}	2.0	0.08 ± 0.08	1.62 ± 0.11	0.411 ± 0.070	Pratt et al. (2009)	P11-LS
L_X–M_{500}	10.0	2.11 ± 0.18	1.34 ± 0.05	0.414 ± 0.044	Mantz et al. (2010b)	M10
L_X–M_{500}	4.0	0.98	1.52	—	Reference	—
M_{500}–Y_X	3.0	1.53 ± 0.04	0.57 ± 0.03	≤ 0.07[b]	Vikhlinin et al. (2009)	V09
M_{500}–Y_X	2.0	1.23 ± 0.02	0.56 ± 0.02	≤ 0.09[c]	Arnaud et al. (2010)	P11-LS
M_{500}–Y_X	10.0	2.25 ± 0.12	0.68 ± 0.04	0.072 ± 0.011	Mantz et al. (2010b)	M10
M_{500}–Y_X	4.0	1.65	0.6	—	Reference	—
$D_A^2 Y_{SZ}$–CY_X	8.0	1.877 ± 0.028	0.916 ± 0.035	0.082 ± 0.035	Rozo et al. (2012a)	V09
$D_A^2 Y_{SZ}$–CY_X	10.0	2.341 ± 0.038	0.828 ± 0.057	0.167 ± 0.039	Rozo et al. (2012a)	P11-LS(z=0.23)
$D_A^2 Y_{SZ}$–CY_X	10.0	2.100 ± 0.09	1.0	≤ 0.15[d]	This work	M10
$D_A^2 Y_{SZ}$–CY_X	10.0	2.303	1.0	—	Reference	

[a]In all cases, we assume the ψ–χ relation takes the form $\langle \ln\psi \rangle = a + \alpha \ln(\chi/\chi_0)$. Our choice of units are $10^{14}\ M_\odot$ for mass, 10^{44} ergs/s for L_X, $10^{14}\ M_\odot$keV for Y_X, and 10^{-5} Mpc^2 for $D_A^2 Y_{SZ}$ and CY_X. Unless otherwise noted, we set χ_0 to the reference scale in the cited work. All scaling relations are evaluated at $z = 0.23$, the median redshift of the maxBCG cluster sample.

[b]Vikhlinin et al. (2009) only state that the scatter is undetectable given the errors on hydrostatic mass estimates, but that this is consistent with 7% scatter as predicted by Kravtsov et al. (2006). We implement this scatter in our analysis as a uniform prior in the variance with the maximum value quoted above.

[c]Arnaud et al. (2007) quote a scatter of 0.087, but provide no error bars. We implement this scatter in our analysis as a uniform prior on the variance using the maximum value quoted above.

[d]Uncertainty in the scatter is implemented as a uniform prior on the variance with the maximum value quoted above. The maximum value is chosen to be close to that derived from the Planck Collaboration (2011b) data by Rozo et al. (2012a).

published L_X-M_{500} relations from 3 independent groups

Rozo et al (2012) arXiv:1204.6292

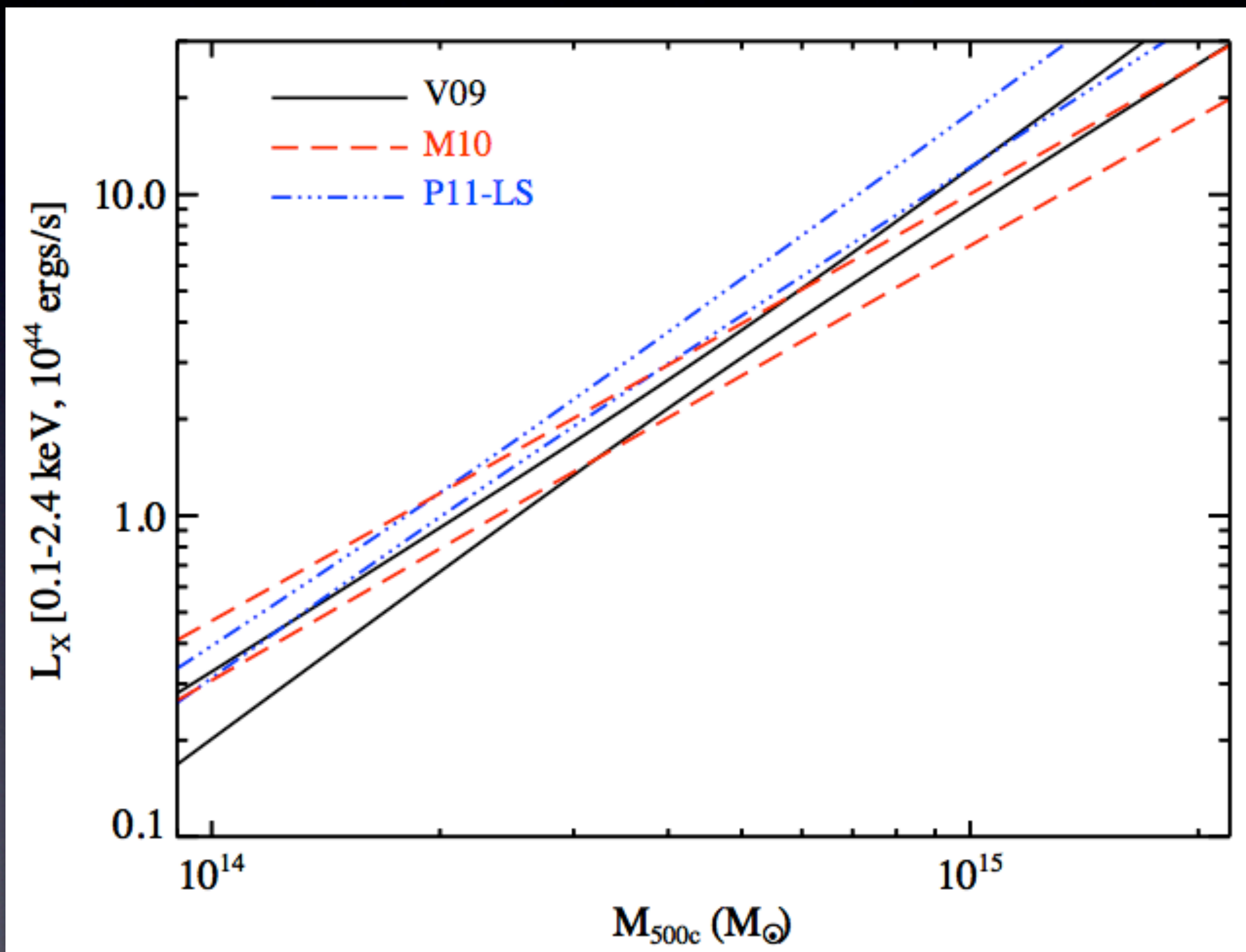

evaluated at z=0.23 assuming self-similar redshift evolution

bands show 68% conf. regions from MC of fits params (slope, intercept, scatter) of power-law mean + log-normal scatter

M10: Mantz et al (2010)
V09: Vihklinin et al (2009)
P11-LS: Planck Coll. (2011)

published L_X-M_{500} relations from 3 independent groups

Rozo et al (2012) arXiv:1204.6292

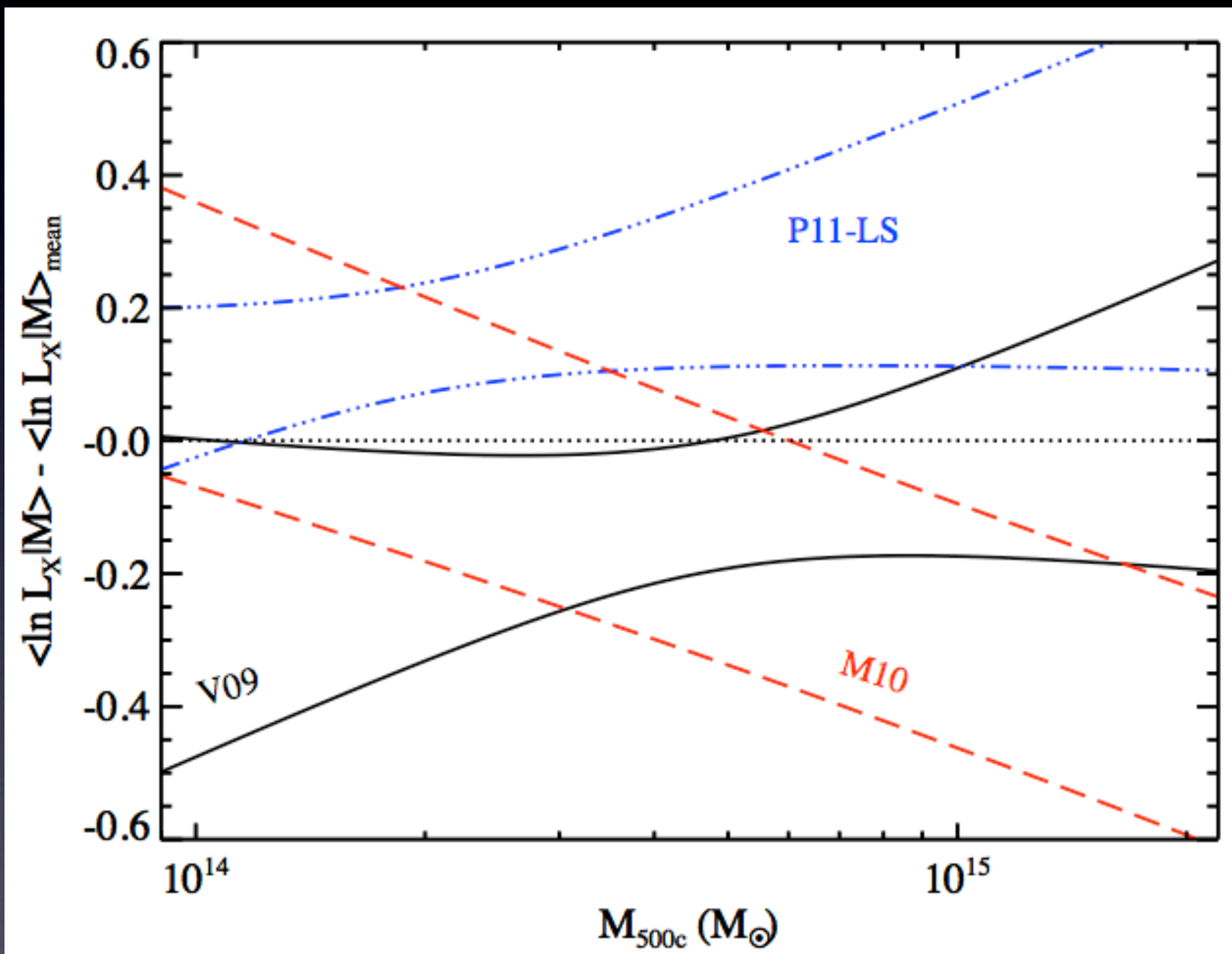

difference view

reference is relation defined by mean slopes and mean intercept at M=4e14

M10: Mantz et al (2010)

V09: Vihklinin et al (2009)

P11-LS: Planck Coll. (2011)

adjusted L_X-M_{500} relations from 3 independent groups

Rozo et al (2012) arXiv:1204.6292

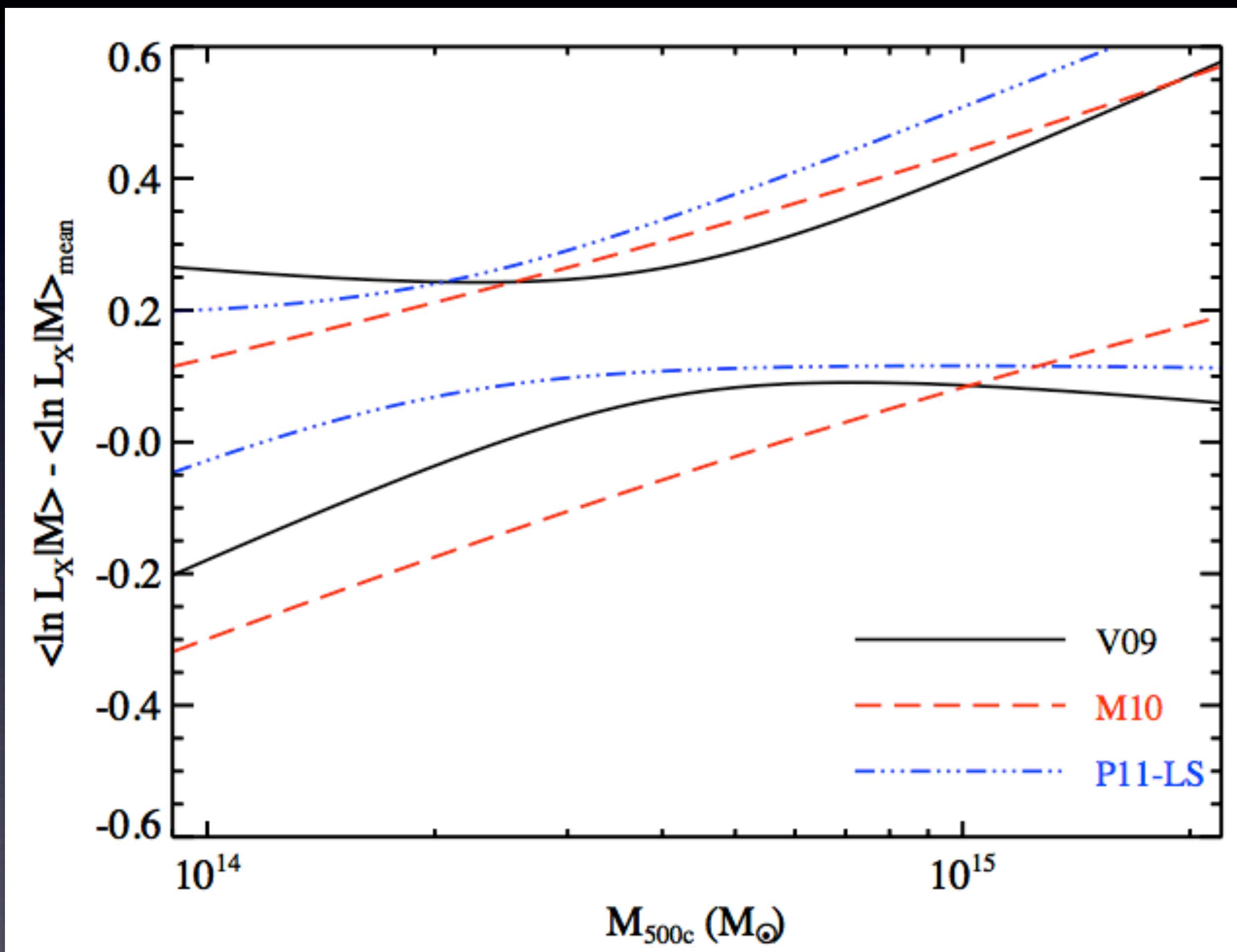

adjusted difference view (same reference)

<u>adjustments</u>:

1) alignment to P11-LS : offsets in Lx, M estimates (paper I) applied to V09 and M10*

2) gas fraction in M10 : fgas = const model changed to fgas~$M^{0.15}$

* M10 total masses also adjusted by –11% due to Chandra recalibration

adjusted M_{500}-Y_X relations from 3 independent groups

Rozo et al (2012) arXiv:1204.6292

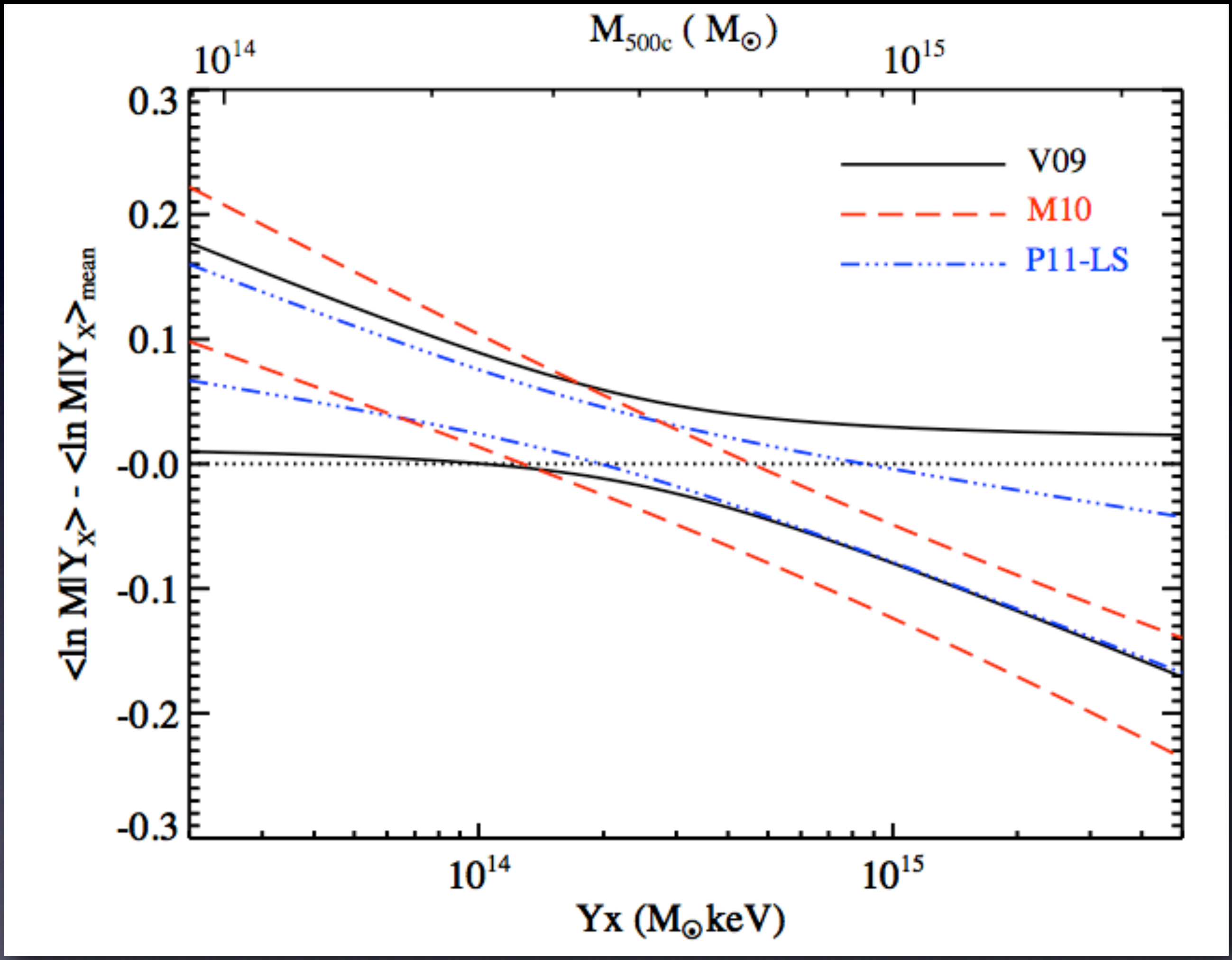

adjusted difference view

<u>adjustments</u>:

1) alignment to P11-LS : offsets in Lx, M estimates (paper I) applied to V09 and M10*

2) gas fraction in M10 : fgas = const model changed to fgas~$M^{0.15}$

* M10 total masses also adjusted by –11% due to Chandra recalibration

toward a unified model for cluster properties

– scaling relations can be aligned by accounting for aperture (mass) bias and other systematics

– simple “plug-n-play” predictions for multi-property scalings are too simplistic if covariance is appreciable and/or selection effects and/or systematic biases are important

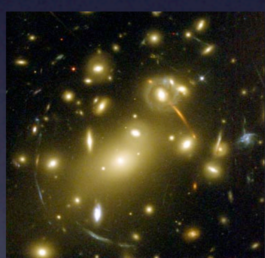

=> M_{lens} = $M_{X\text{-ray}}$ =>

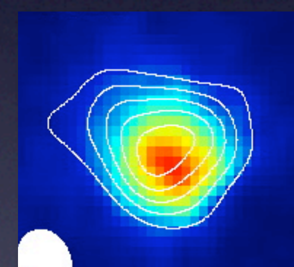

optical Ngal	**lensing mass**	**X-ray hydrostatic mass**	**thermal SZ amplitude**

a multivariate log-normal model for massive halo properties

1 A Local Model for Multivariate Counts

Consider a mass function described locally as a power-law in mass with slope $-\alpha$. Specifically, using $\mu \equiv \ln M$, define the mass function, $n(\mu, z)$, as the likelihood of finding a halo at redshift z in the mass range μ to $\mu + d\mu$ within a small comoving volume dV,

$$dp \equiv n(M, z)\, d\ln M\, dV = AM^{-\alpha} d\ln M\, dV = A\, e^{-\alpha\mu}\, d\mu\, dV. \quad (1)$$

piecewise power-law mass function; alpha is local slope d(logn)/d(logM)

The local slope, α, and amplitude, A, implicitly depend on mass and redshift in a manner dependent on cosmology (*e.g.*, Tinker et al. 2008).

Consider a set of N halo properties, $S_i \in \{N_{\rm gal}, L_{\rm X}, T_{\rm X}, M_{\rm gas}, Y_{\rm X}, Y_{\rm SZ}, \cdots\}$, let $\mathbf{s}$ be a vector containing their logarithms,

$$s_i = \ln(S_i) \quad (2)$$

Assume that the mass scaling behavior of these properties are power-laws, so that the mean ln(signal) for a mass–complete sample scales as

$$\bar{\mathbf{s}}(\mu, z) = \mathbf{m}\mu + \mathbf{b}(z). \quad (3)$$

assumed form of property-mass relation

The elements of vector $\mathbf{m}$ are the slopes of the individual mass-observable relations. (Note that, at some fixed epoch, we can always choose units such that the intercepts $b_i(z) = 0$.)

Assume that ln(signal) deviations about the mean are Gaussian, described by a likelihood

$$p(\mathbf{s}|\mu) = \frac{1}{(2\pi)^{N/2}|\Psi|^{1/2}} \exp\left[-\frac{1}{2}(\mathbf{s} - \bar{\mathbf{s}})^\dagger \Psi^{-1} (\mathbf{s} - \bar{\mathbf{s}})\right], \quad (4)$$

where the covariance matrix has elements

$$\Psi_{ij} \equiv \langle (s_i - \bar{s}_i)(s_j - \bar{s}_j) \rangle, \quad (5)$$

and the brackets denote an ensemble average over a (large) mass–complete sample.

explicit form for local counts as a function of multiple properties

1.1 Multivariate Space Density

The space density as a function of the multivariate properties, $\mathbf{s}$, is found by the convolution, $n(\mathbf{s}) = \int d\mu\, n(\mu)\, p(\mathbf{s}|\mu)$. Using equations (1) and (4), the result is

$$n(\mathbf{s}) = \frac{A\Sigma}{(2\pi)^{(N-1)/2}|\Psi|^{1/2}} \exp\left[-\frac{1}{2}(\mathbf{s}^\dagger\Psi^{-1}\mathbf{s} - \frac{\bar{\mu}^2(\mathbf{s})}{\Sigma^2})\right], \qquad (6)$$

exact form for multi-property space density

where Σ^2 is the **multi-property mass variance** defined by

$$\Sigma^2 = (\mathbf{m}^\dagger\Psi^{-1}\mathbf{m})^{-1}, \qquad (7)$$

and the mean mass is

$$\bar{\mu}(\mathbf{s}) = \frac{\mathbf{m}^\dagger\Psi^{-1}\mathbf{s}}{\mathbf{m}^\dagger\Psi^{-1}\mathbf{m}} - \alpha\Sigma^2, \qquad (8)$$

$$\equiv \bar{\mu}_0(\mathbf{s}) - \alpha\Sigma^2. \qquad (9)$$

mean mass selected by signals is biased low (Malmquist bias)

The first term, $\bar{\mu}_0(\mathbf{s})$, is the mean mass for the case of a flat mass function, $\alpha = 0$, which corresponds to the mass expected from inverting the input log-mean relation.

The second term, $\alpha\Sigma^2$, represents the mass shift induced by asymmetry in the convolution when $\alpha > 0$. (Low mass halos scattering up outnumber high mass systems scattering down.) Note that **the magnitude of this effect scales with the variance**, not the rms deviation.

Applying Bayes' theorem in the form $p(\mu|\mathbf{s}) = p(\mathbf{s}|\mu)n(\mu)/n(\mathbf{s})$ leads to the result that the set of masses selected by a specific set of properties is Gaussian in the log with mean given by equation (9) and variance, equation (7).

simple case of one property

1.1.1 Explicit expressions for the one-variable case

For a single property, $s \equiv \ln(S)$, with slope, m, and logarithmic scatter at fixed mass, σ, the mass variance at fixed S is

$$\Sigma^2 = \left(\frac{\sigma}{m}\right)^2. \tag{10}$$

The mean mass for a sample complete in S is

$$\bar{\mu}(s) = \frac{s}{m} - \alpha\Sigma^2. \tag{11}$$

The property space density function is

$$n(s)\,ds = (A/m)\,\exp\{-\alpha\left(\frac{s}{m} - \alpha\Sigma^2/2\right)\}\,ds, \tag{12}$$

which is a power-law in the original property, $n(S) \propto S^{-(\alpha/m)}$.

Note that the effective shift in mass, $\alpha\Sigma^2/2$, is half that in the expression above. These expressions are consistent, in that they address different questions. Equation (11) gives the mean ln(mass) of a signal-selected sample while equation (12) gives the ln(mass) value that matches the local space density – in number per volume per ln(S) – of halos with property value, S.

cosmology

astrophysics

two properties

1.1.2 Explicit expressions for the two-variable case

For two properties, we introduce the correlation coefficient, $r \equiv \langle \delta_1 \delta_2 \rangle$, of the normalized deviations, $\delta_i \equiv (s_i - \bar{s}_i)/\sigma_i$, and write the covariance matrix,

$$\Psi = \begin{pmatrix} \sigma_1^2 & r\sigma_1\sigma_2 \\ r\sigma_1\sigma_2 & \sigma_2^2 \end{pmatrix},$$

and its inverse,

$$\Psi^{-1} = (1-r^2)^{-1} \begin{pmatrix} \frac{1}{\sigma_1^2} & -\frac{r}{\sigma_1\sigma_2} \\ -\frac{r}{\sigma_1\sigma_2} & \frac{1}{\sigma_2^2} \end{pmatrix}.$$

The mass variance is now a harmonic mixture

$$\Sigma^{-2} = (1-r^2)^{-1} \left(\sigma_{\mu 1}^{-2} + \sigma_{\mu 2}^{-2} - 2r\sigma_{\mu 1}^{-1}\sigma_{\mu 2}^{-1} \right), \tag{13}$$

where $\sigma_{\mu i} = \sigma_i/m_i$ is the mass scatter at fixed signal S_i.

The zero-slope mean mass is

$$\bar{\mu}_0(s_1, s_2) = \frac{(s_1/m_1)\sigma_{\mu 1}^{-2} + (s_2/m_2)\sigma_{\mu 2}^{-2} - r(s_1/m_1 + s_2/m_2)\sigma_{\mu 1}^{-1}\sigma_{\mu 2}^{-1}}{\sigma_{\mu 1}^{-2} + \sigma_{\mu 2}^{-2} - 2r\sigma_{\mu 1}^{-1}\sigma_{\mu 2}^{-1}}, \tag{14}$$

and the **joint space density** is

$$n(s_1, s_2) = \frac{A\Sigma}{\sqrt{2\pi(1-r^2)}\sigma_1\sigma_2} \exp\left[-\alpha\bar{\mu}_0 + \frac{\Sigma^2}{2} \left(\alpha^2 - \frac{(s_1/m_1 - s_2/m_2)^2}{\sigma_{\mu 1}^2 \sigma_{\mu 2}^2} \right) \right]. \tag{15}$$

The first two terms in the exponent are analogous to those in the 1D expression, equation (12). For "reasonable" choices of (S_1, S_2) pairs — meaning values that pick out comparable mass scales, $s_1/m_1 \sim s_2/m_2$ — the space density remains effectively power-law. The third term in the exponent suppresses the number density for unreasonable pairings of s_1/m_1 and s_2/m_2, those lying out in the wings of the bivariate Gaussian.

anti-correlated signals best for mass selection

mass scatter for two-property joint selection

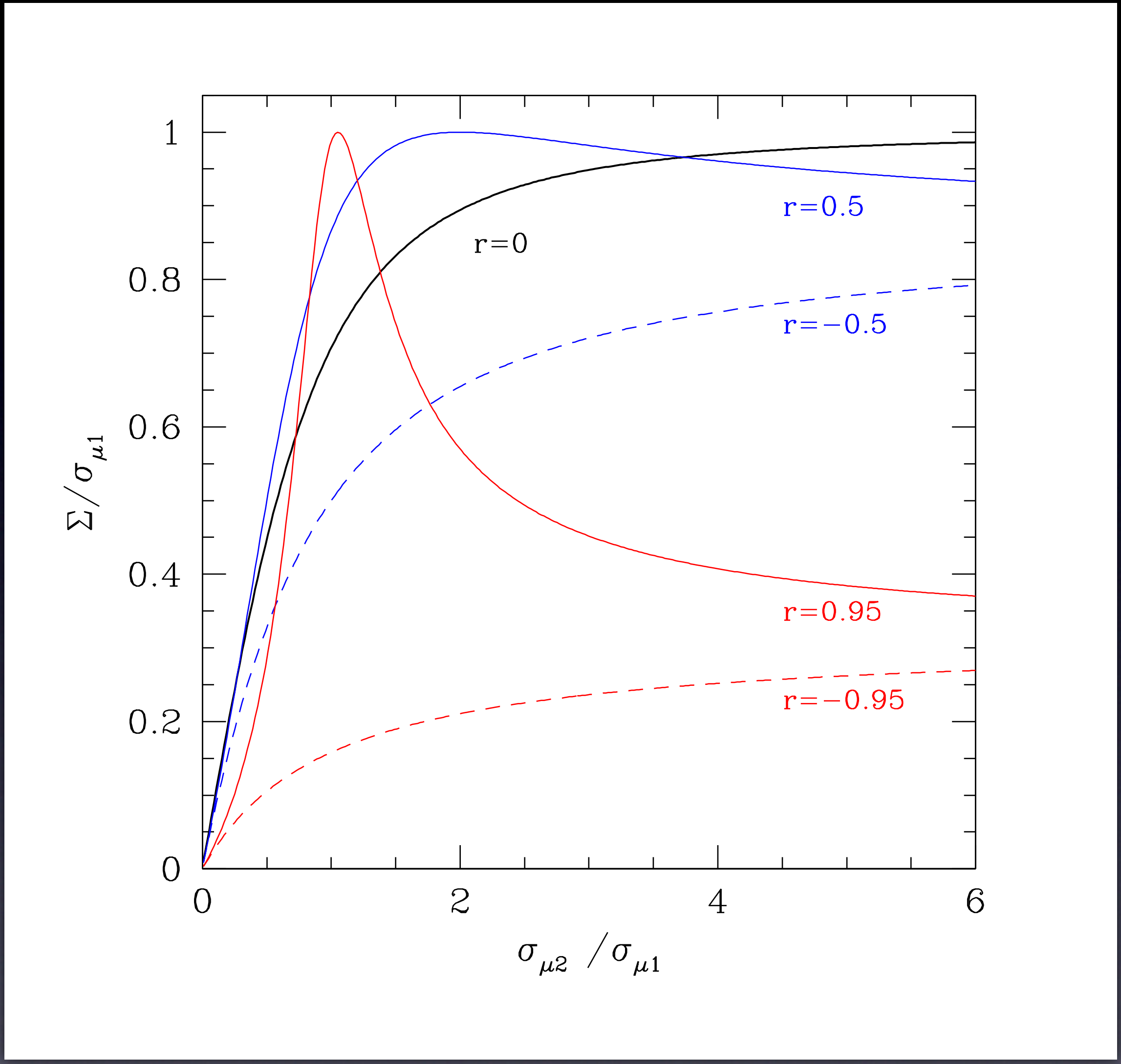

effects of selection

1.2 Property-selected samples

For a halo sample selected with some property, s_1, we can now use Bayes' theorem to find the joint probability of those halos having a second property, s_2, and mass, μ. The result can be expressed as a bivariate Gaussian in terms of the two-element vector, $\mathbf{t} = [s_2\ \mu]$,

$$p(\mathbf{t}|s_1) \;=\; \frac{1}{(2\pi)|\tilde{\Psi}|^{1/2}} \exp\left[-\frac{1}{2}(\mathbf{t}-\bar{\mathbf{t}})^\dagger \tilde{\Psi}^{-1}(\mathbf{t}-\bar{\mathbf{t}})\right], \tag{16}$$

where the mean mass, $\bar{\mu}(s_1)$, is defined by equation (11) and the mean of the non-selection property is given by

$$\bar{s}_2(s_1) \;=\; m_2\left(\bar{\mu}(s_1) + \alpha r \sigma_{\mu 1}\sigma_{\mu 2}\right). \tag{17}$$

Note that, if $r < 0$, the non-selected property mean can be "doubly" biased low relative to a simple $m_2(s_1/m_1)$ expectation, with one shift coming from the extra $(-\alpha\Sigma^2)$ term in the mean mass and the second coming from the second term in the above expression.

The covariance in s_2 and μ at fixed s_1 is given by

$$\tilde{\Psi} = \begin{pmatrix} \sigma_{21}^2 & \tilde{r}\sigma_{21}\sigma_{\mu 2} \\ \tilde{r}\sigma_{21}\sigma_{\mu 2} & \sigma_{\mu 2}^2 \end{pmatrix},$$

where the variance in s_2 at fixed s_1 is

$$\sigma_{21}^2 \;=\; m_2^2\left(\sigma_{\mu 1}^2 + \sigma_{\mu 2}^2 - 2r\sigma_{\mu 1}\sigma_{\mu 2}\right). \tag{18}$$

<u>future program</u>: combine large samples to extract signal covariance

mean of 2nd property for sample selected on 1st property

variance in 2nd property

RASS X-ray stacking analysis of maxBCG sample

Rykoff et al 2008

variance in Lx at fixed Ngal $\sigma_{\ln L_X \mid N_{gal}} = 0.83 \pm 0.03$

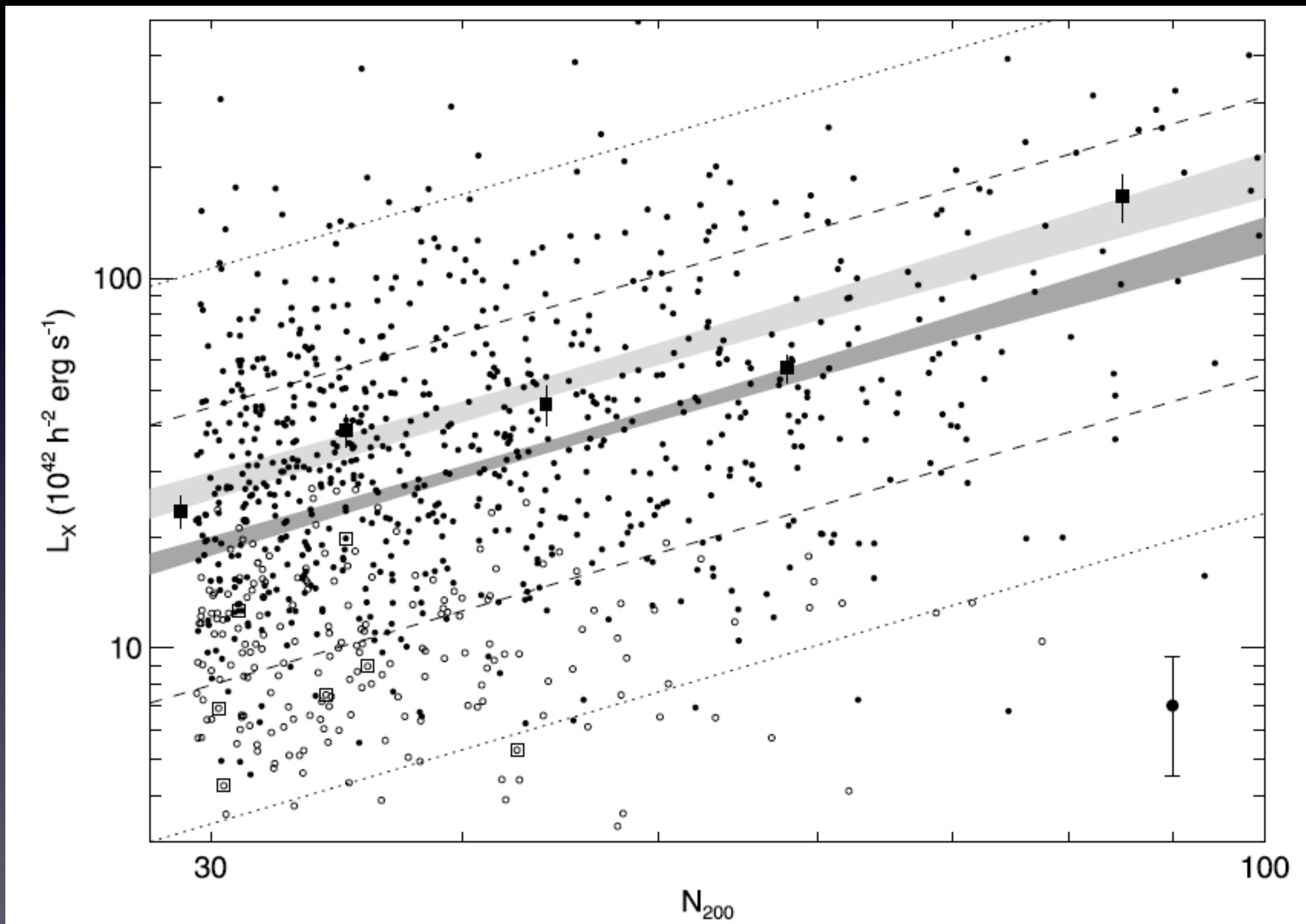

model exercise to derive Ysz-M scaling

Rozo et al (2012) arXiv:1204.6292

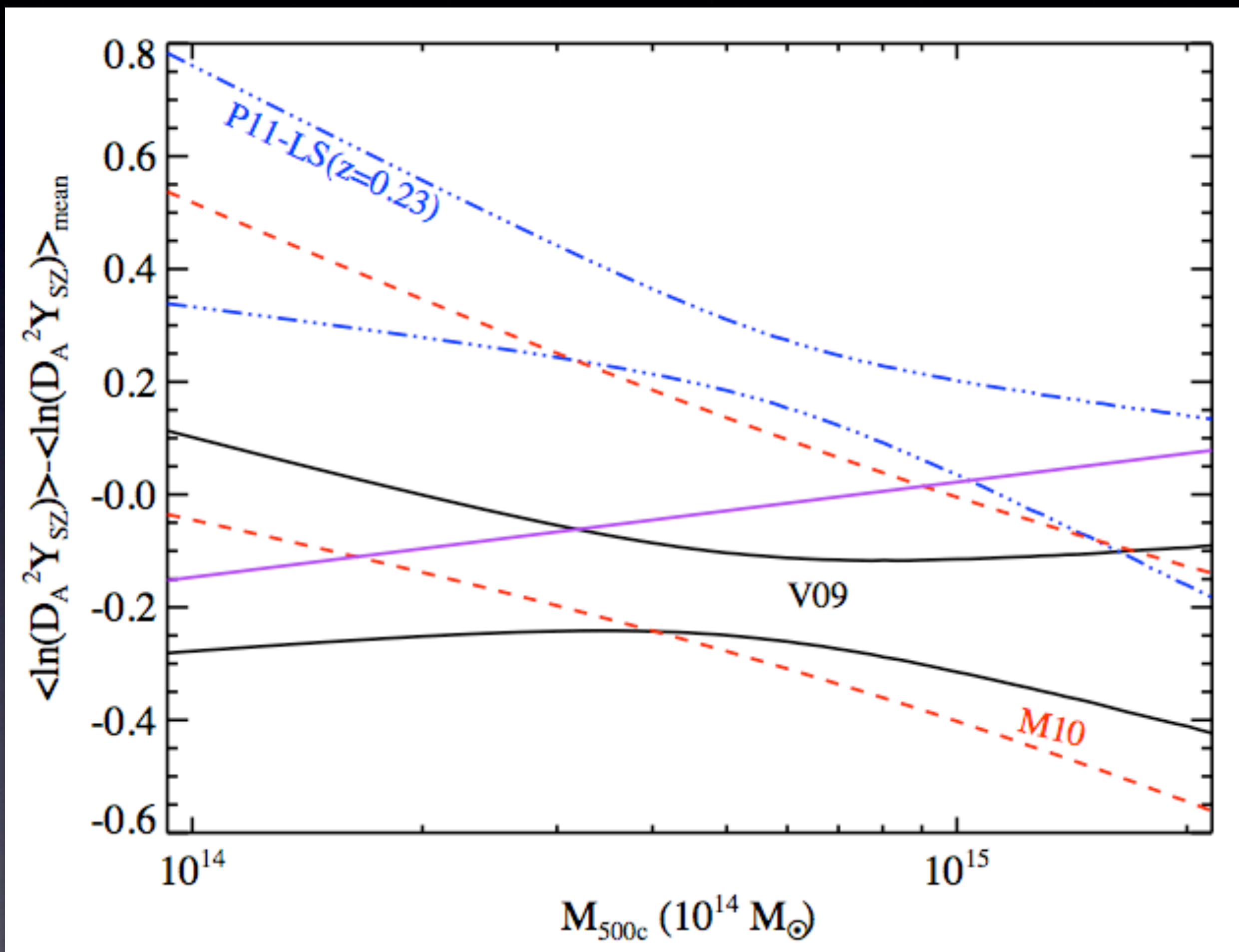

Use model to combine published relations for
<M | Yx> and
<Ysz | Yx>
to derive
<Ysz | M>

difference view using reference w/ self-similar slope (5/3) and mean amplitude of 3 works

P11-LS (z=0.23) uses Ysz-Yx for 0.13<z<0.3 only (maxBCG z-range)

magenta line gives full sample result

additional constraint from number counts (`abundance matching')

Rozo et al (2012) arXiv:1204.6292

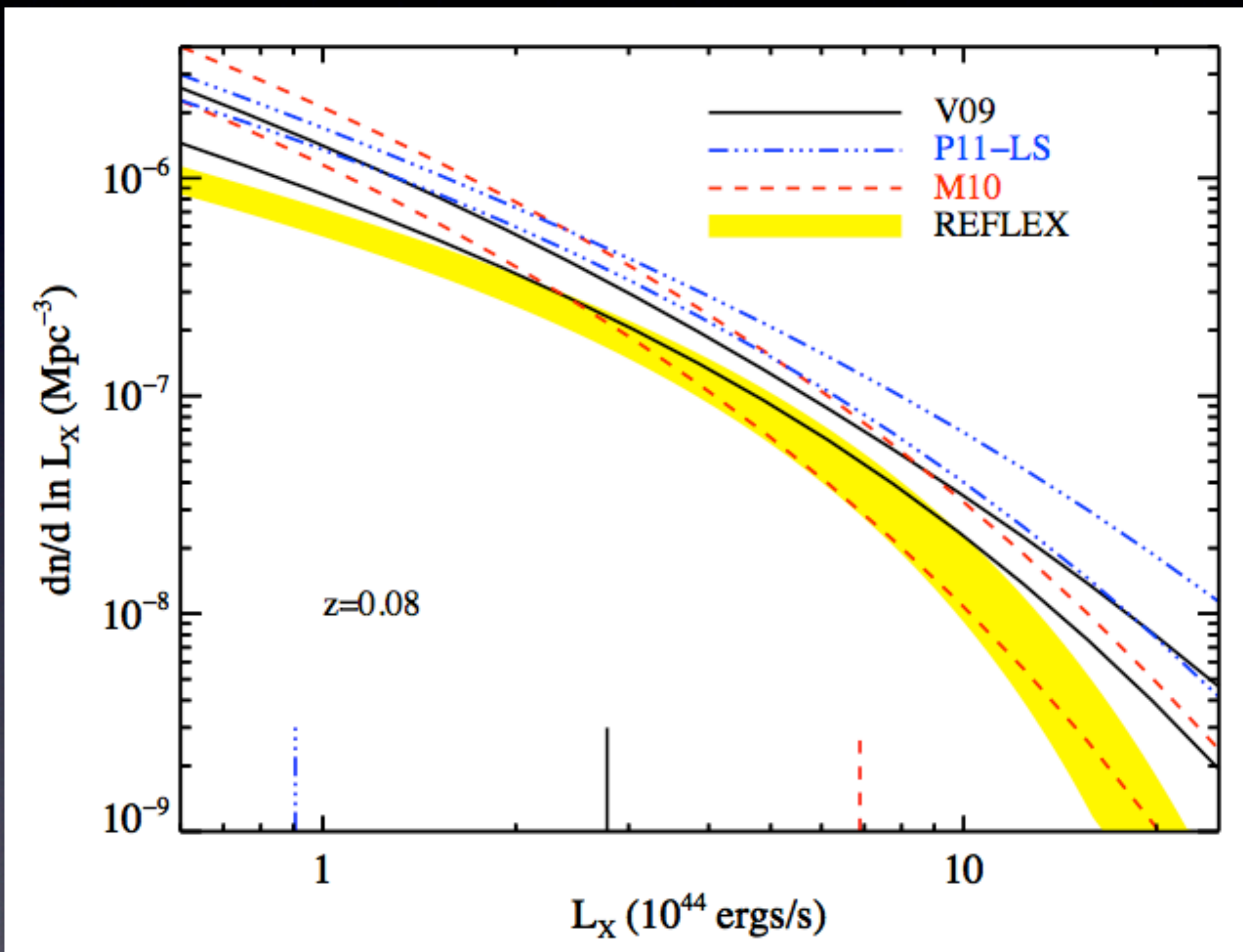

Use WMAP7 halo mass function convolved with published Lx-M relations

Compare to X-ray luminosity function published for the local REFLEX sample (median z = 0.08)

paper II summary

- published X-ray scalings have moderate tension that improves after aperture + other bias adjustments

- we introduce a power-law plus log-normal covariance model for multiple cluster properties (including true mass) as an improvement to direct substitution of mean relations
  – corrections for means may depend on local slope of mass function
  – scatter in property B includes covariance with selection property A

- abundance constraint adds additional constraining power
  – largest tension with P11-LS Lx-M scaling

paper III:
closing the loop -
a return to the
Planck maxBCG result

mis-centering of optical clusters is a 10-30% effect

Rozo et al (2012) arXiv:1204.6305

Biesiadzinski, T. et al (2012) arXiv:1201.1282B

TABLE 1
Y_{SZ}–N_{200} DATA

N_{200}	$D_A^2 Y_{SZ}/(10^{-5}\ \mathrm{Mpc}^{-2})$	Centering Correction
10– 13	0.058± 0.012	0.74± 0.13
14– 17	0.107± 0.020	0.77± 0.11
18– 24	0.222± 0.028	0.80± 0.08
25– 32	0.394± 0.044	0.82± 0.08
33– 43	0.692± 0.074	0.84± 0.07
44– 58	1.205± 0.130	0.86± 0.07
59– 77	1.876± 0.241	0.87± 0.07
78– 104	4.594± 1.009	0.89± 0.09

[a] The data in the first two columns is from Planck Collaboration (2011c, P11-opt), after being corrected for the effects of cluster miscentering following Biesiadzinski et al. (2012) (third column). The uncertainty in the corrections is added in quadrature to the observational errors.

maxBCG lensing analysis includes estimate of mis-centering derived from ADDGALS-based mock catalogs

Biesiadzinski et al use this model to simulate effect of mis-centering on SZ measurements

Ysz-N200 scalings using scaling results from paper II

Rozo et al (2012) arXiv:1204.6305

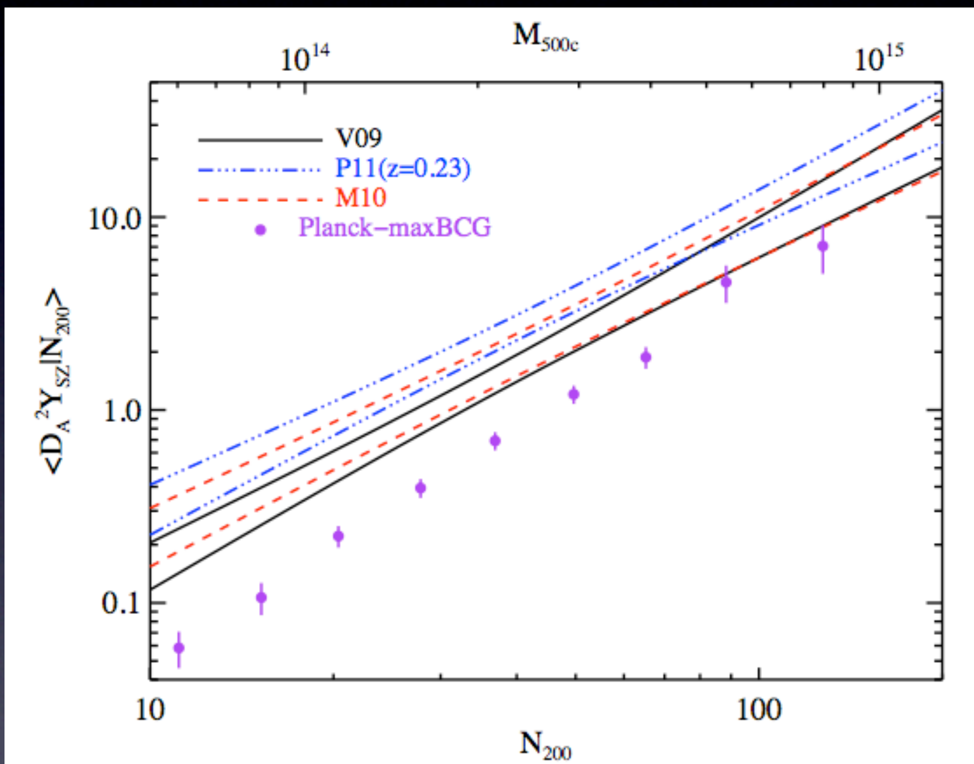

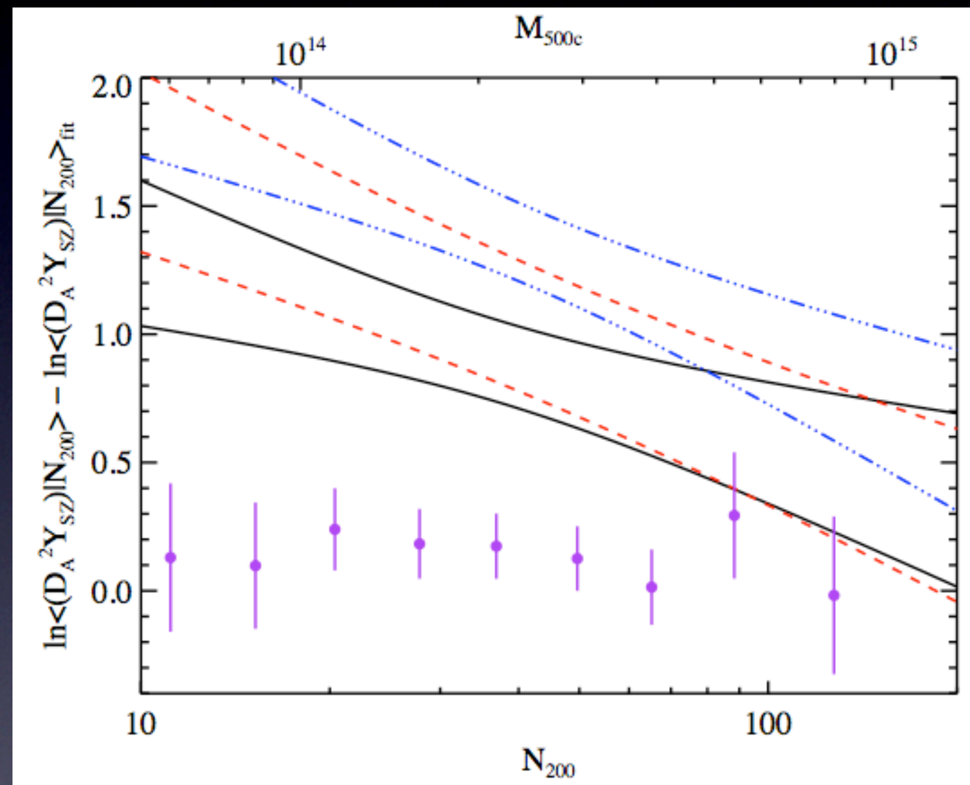

- Planck measurements corrected for mis-centering
- reference used in RHS is published Planck observed relation
- all models are in tension with the observations

Ysz-N200 scalings : potential resolution

Rozo et al (2012) arXiv:1204.6305

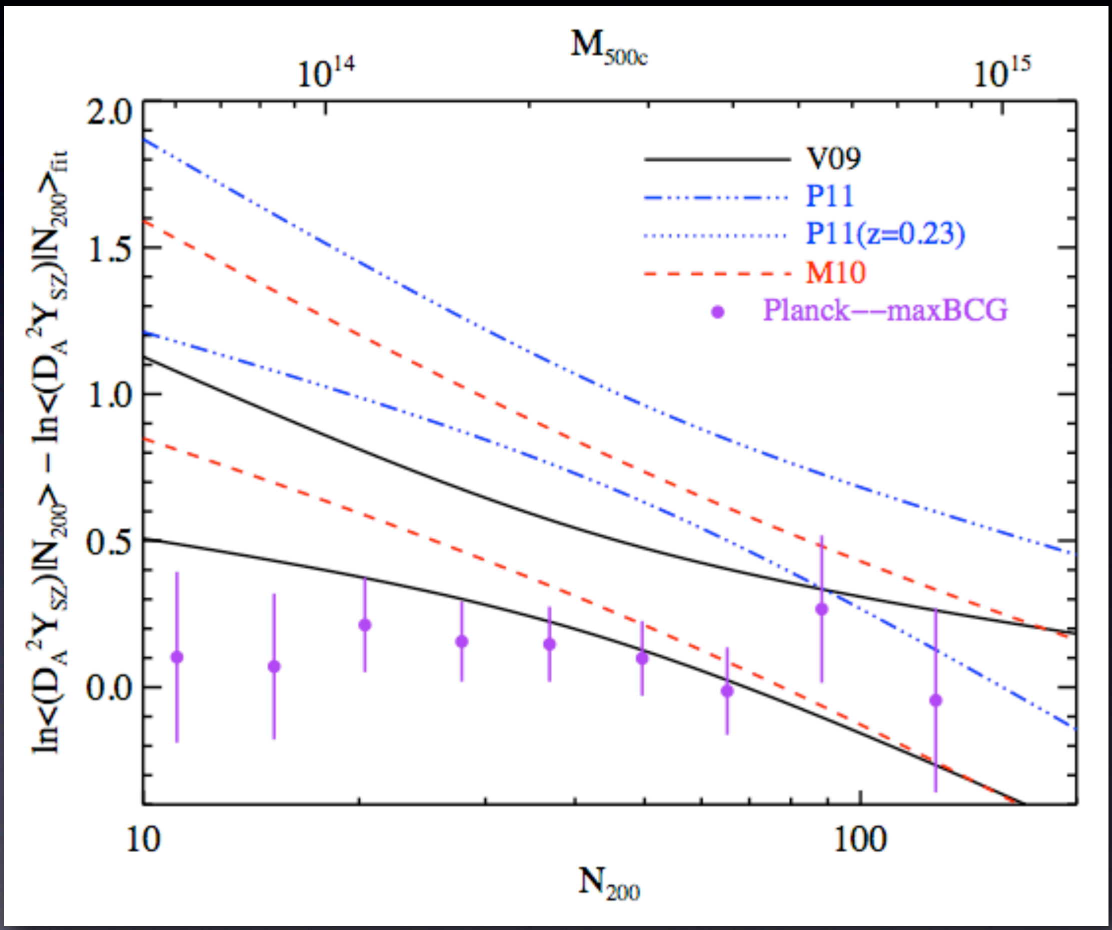

Proposed resolution:

mass estimate biases

– 15% (21% at R500) bias in hydrostatic masses (estimates are biased low)

– 10% reduction in maxBCG lensing masses measurements published in Rozo et al (2009) (~1sigma systematic error)

recent hydrostatic mass bias from gas dynamic simulations

Sembolini et al (2012) arXiv:1207.4438

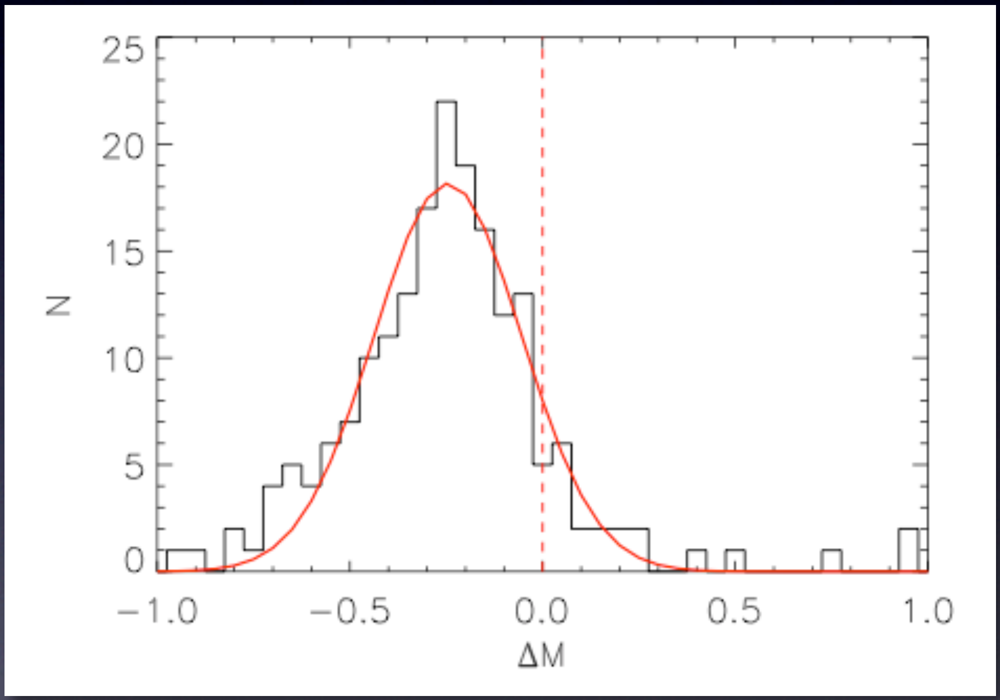

Marenostrum-MultiDark SImulations (MUSIC)

histogram of fractional error
$(M_{HS} - M_{true}) / M_{true}$
using 3D information

ALL simulations studies have shown this effect (since Evrard 1990 with ~500 particles/halo !)

proposed `compromise' scaling relations

Rozo et al (2012) arXiv:1204.6305

TABLE 4
PREFERRED SET OF SCALING RELATIONS

Relation	χ_0	Amplitude ($a_{\psi\|\chi}$)	$\alpha_{\psi\|\chi}$	$\sigma_{\ln\psi\|\chi}$	Sample
L_X–M	4.4	0.72 ± 0.07 $(ran) \pm 0.16$ (sys)	1.55 ± 0.09	0.39 ± 0.03	V09+maxBCG
$D_A^2 Y_{SZ}$–M	4.4	0.87 ± 0.06 $(ran) \pm 0.17$ (sys)	1.71 ± 0.08	0.15 ± 0.02	V09+maxBCG
M–N_{200}	40	0.75 ± 0.10	1.06 ± 0.11	0.45 ± 0.10	maxBCG
L_X–N_{200}	40	0.04 ± 0.10	1.63 ± 0.08	0.83 ± 0.10	maxBCG
Y_{SZ}–N_{200}	40	-0.24 ± 0.20	1.97 ± 0.10	0.70 ± 0.15	maxBCG
Y_{SZ}–L_X	1.0	-0.29 ± 0.06	1.10 ± 0.03	0.40 ± 0.05	P11-X

[a] X-ray luminosity is measured in the $[0.1, 2.4]$ keV band in units of 10^{44} ergs/s. $D_A^2 Y_{SZ}$ is in units of 10^{-5} Mpc^2. The maxBCG scaling relations are bias-corrected, while the V09+maxBCG relations are the joint constraint from the bias-corrected V09 and maxBCG samples. Scaling relations involving mass include a $\pm10\%$ systematic uncertainty in the mass. The error in the amplitude of the Y_{SZ}–L_X relation is larger than that quoted in P11-X because we include the uncertainty in our systematic corrections. This set of scaling relations is fully self-consistent.

abundance test of preferred scalings

Rozo et al (2012) arXiv:1204.6305

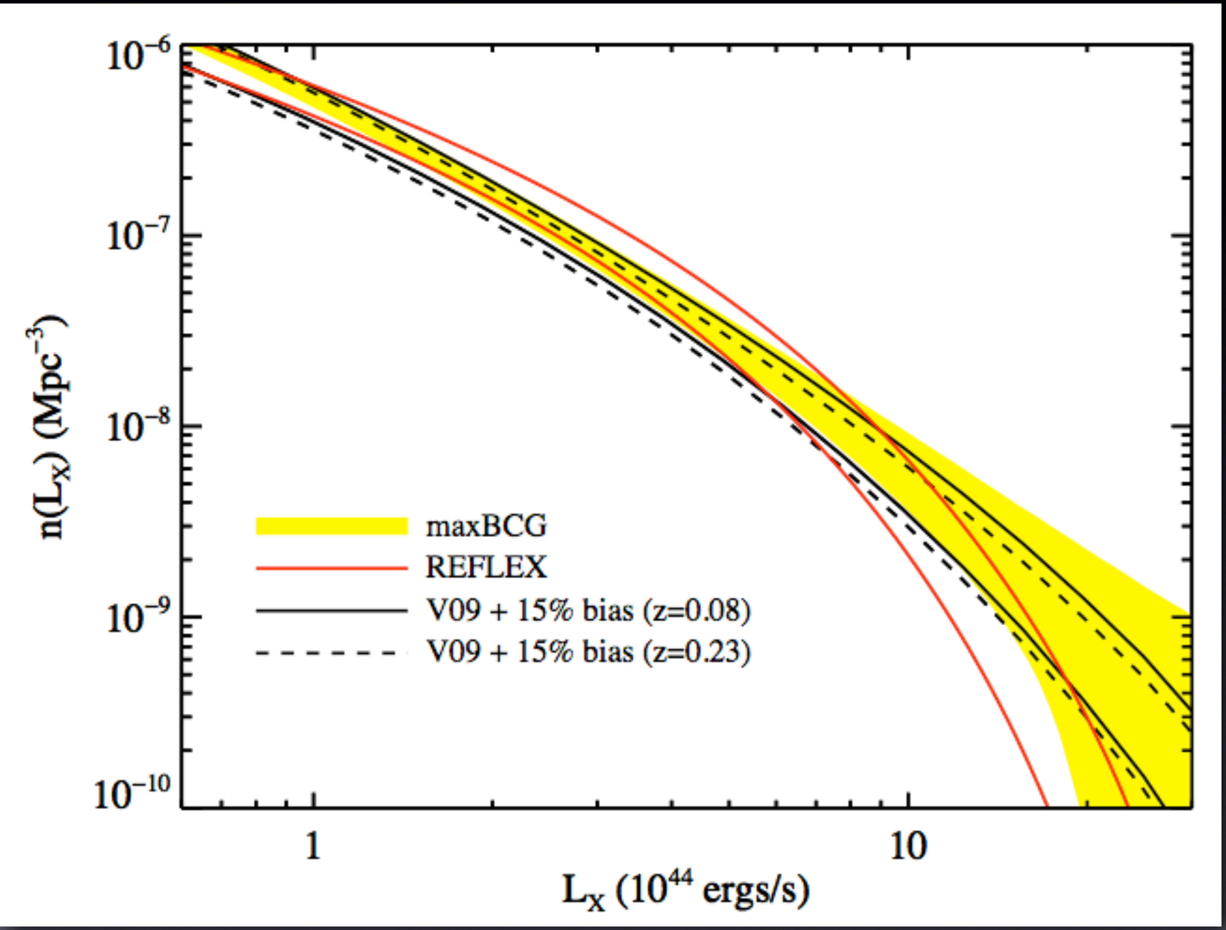

<u>consistency check</u>:

– maxBCG number counts convolved with Lx-N200 relation

– halo mass function convolved with V09 (adjusted) Lx-M relation

comparison to other observed Lx-M scaling relations

Rozo et al (2012) arXiv:1204.6305

TABLE 6
MASS OFFSET BETWEEN OUR PREDICTED MASSES AND VALUES FROM THE LITERATURE

Work	$\ln \langle M \| L_X \rangle - \ln M_{lit}$	No. of Clusters in Sample
V09 ($z \leq 0.3$)	0.11 ± 0.04	49
V09 ($z > 0.3$)	0.22 ± 0.05	36
M10	0.02 ± 0.03	95
P11 ($z \leq 0.13$)	0.09 ± 0.05	24
P11 ($z > 0.13$)	0.21 ± 0.04	38
Okabe et al. (2010)	0.53 ± 0.07	21
Mahdavi et al. (2008)	0.22 ± 0.12	11
Hoekstra et al. (2011)	0.13 ± 0.13	25
Umetsu et al. (2011)	-0.42 ± 0.14	5

[a] Mean mass offset between our predicted masses using L_X, and those reported in the literature. All means are inverse-variance weighted.

paper III summary

- the Planck Ysz-N200 stacked scaling discrepancy can be resolved by a combination of
  - biases in hydrostatic (~20%) and lensing (~10%) mass estimates
  - mis-centering of optically selected clusters from halo/gas centers

- a set of compromise scaling relations (power-law plus log-normal scatter) are proposed for several relations involving {M, Lx, N200, Ysz}

- abundance constraint demonstrates internal consistency of these relations

- tensions with some published Lx-M relations are identified